The Abdus Salam
International Centre for Theoretical Physics

United Nations
Educational, Scientific
and Cultural Organization

International Atomic
Energy Agency

H4.SMR/1775-21

"8th Workshop on Three-Dimensional Modelling of
Seismic Waves Generation, Propagation and their Inversion"

25 September - 7 October 2006

Focal mechanisms from fluid induced seismicity

F. H. Cornet

Institute de Physique du Globe de Paris
France

Focal mechanisms from fluid induced seismicity

The borehole site configuration

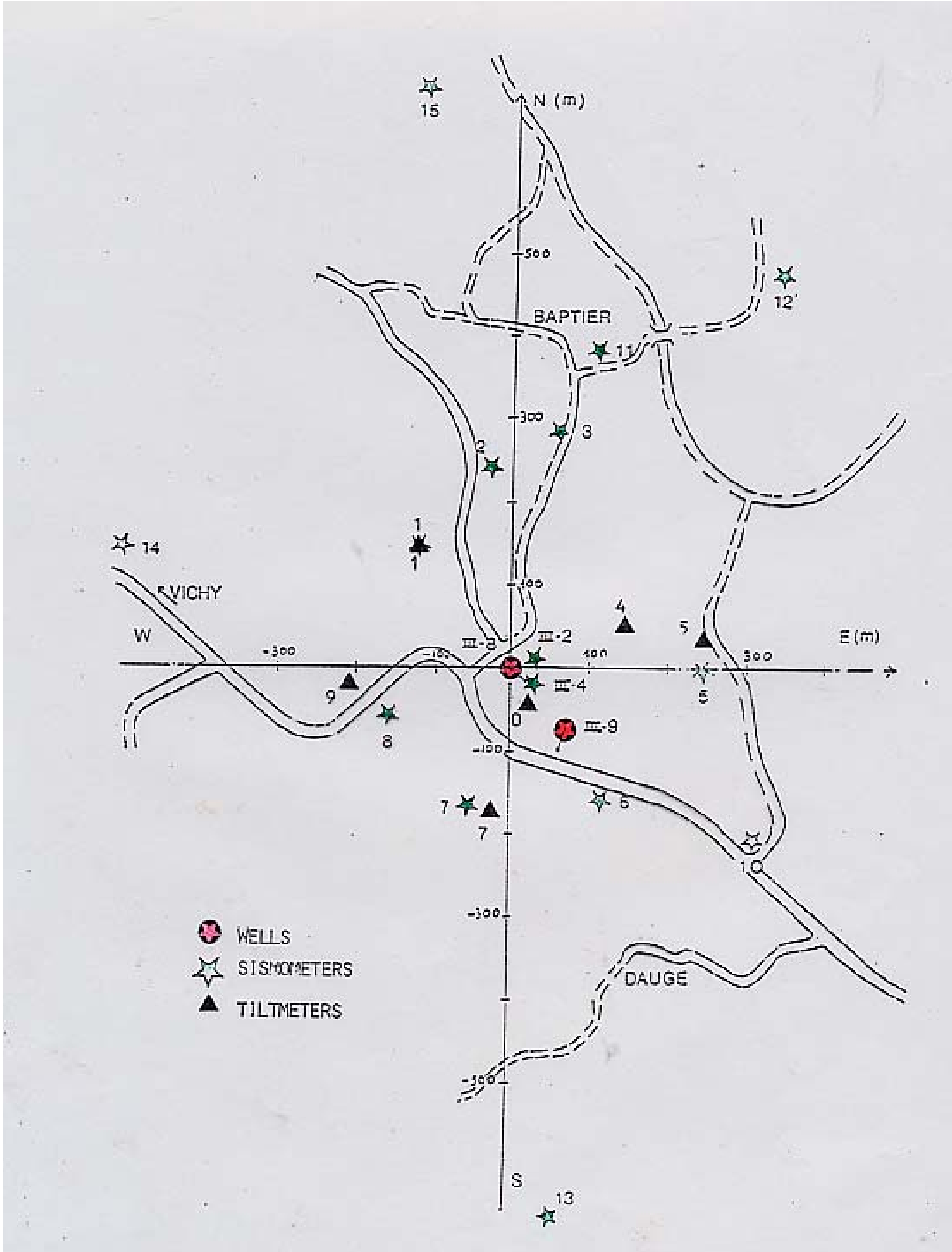

Stress field determination from hydraulic testing

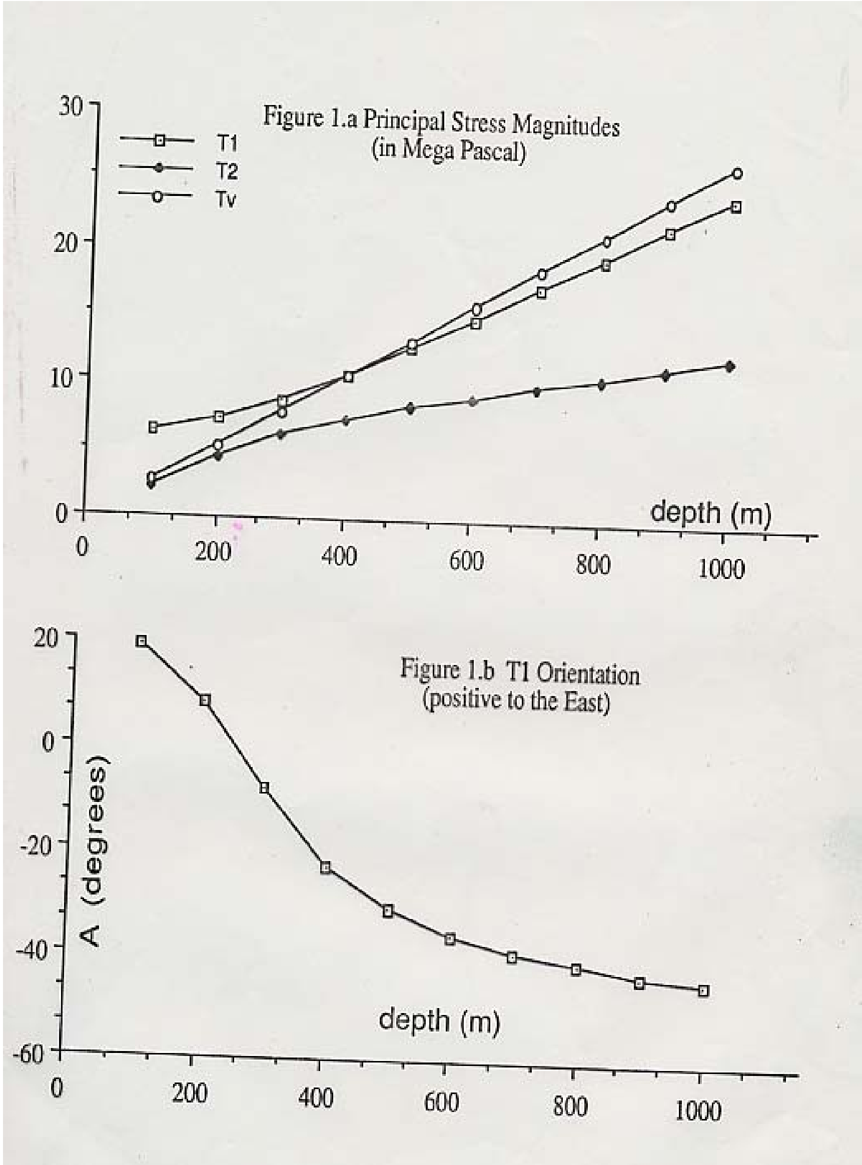

Location of induced microseismicity

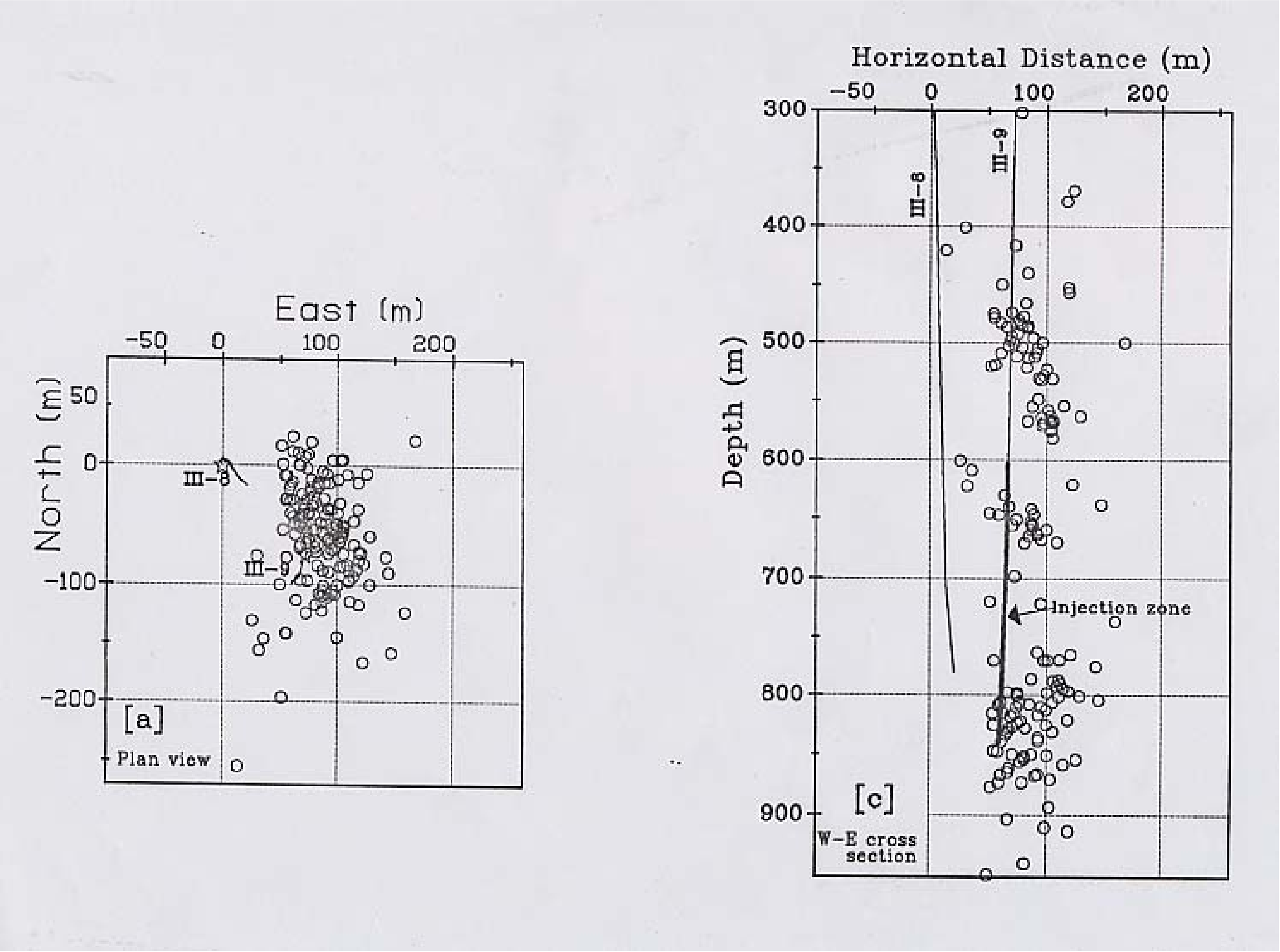

Observed focal mechanisms

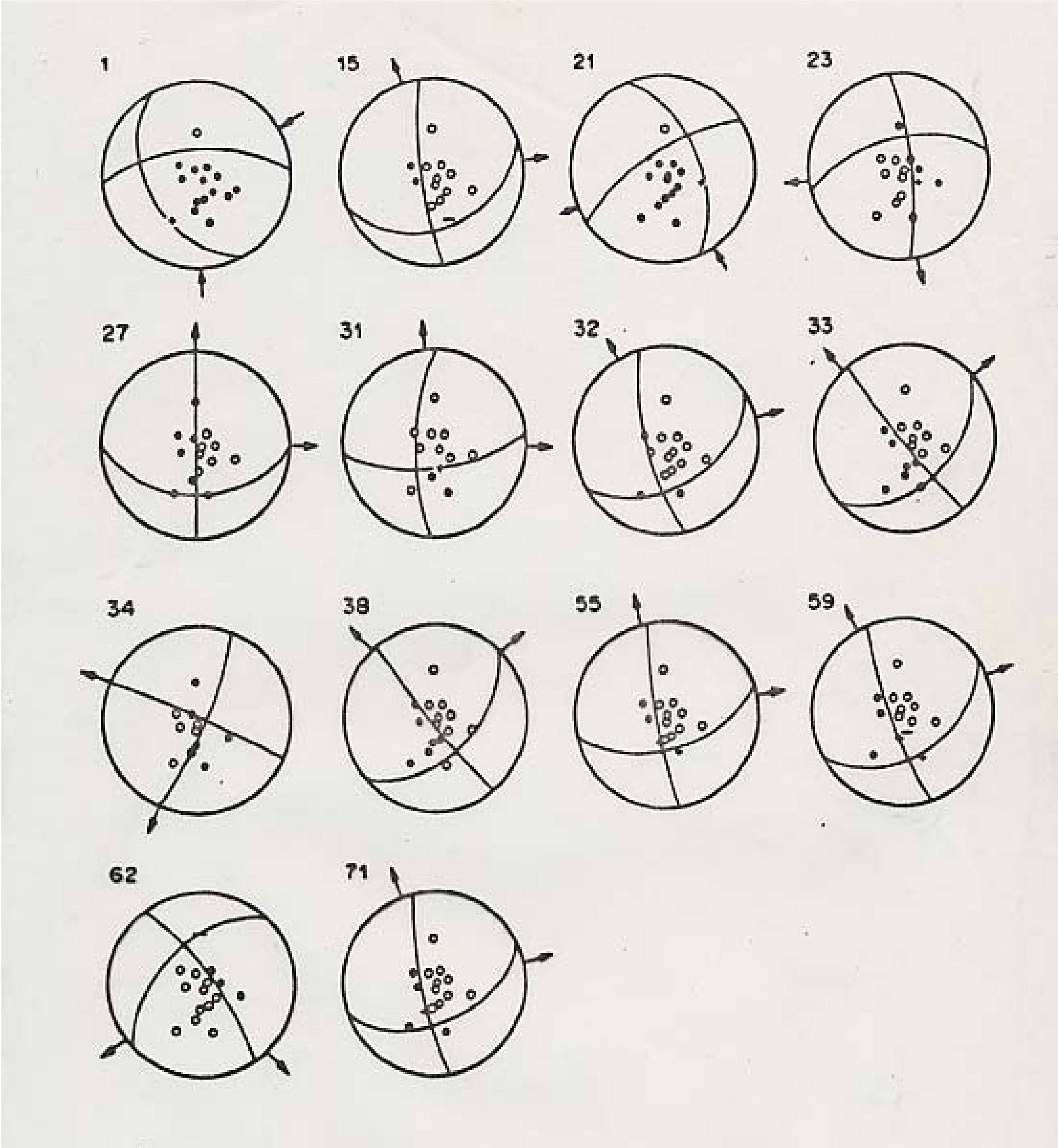

Joint inversion of focal mechanisms and hydraulic tests

Definition of the Problem

For all focal plane solutions , the resolved shear stress on fault plane (τ) is assumed parallel to the unit slip vector (**s**) :

$$\mathbf{s} \cdot \tau / |\tau| = 1$$

HTPF data provides direct measurement of normal stress σ_n supported by pre-existing fractures of known orientation **n** :

$$\sigma_n = \sigma(x)\,\mathbf{n}.\mathbf{n}$$

Find stress field σ (x) which varies linearly with depth and which fits best both sets of data ;

$$\sigma(x) = \mathbf{S} + z\alpha$$

S defined by 6 components,
α defined by 4 components.

Integrated inversion

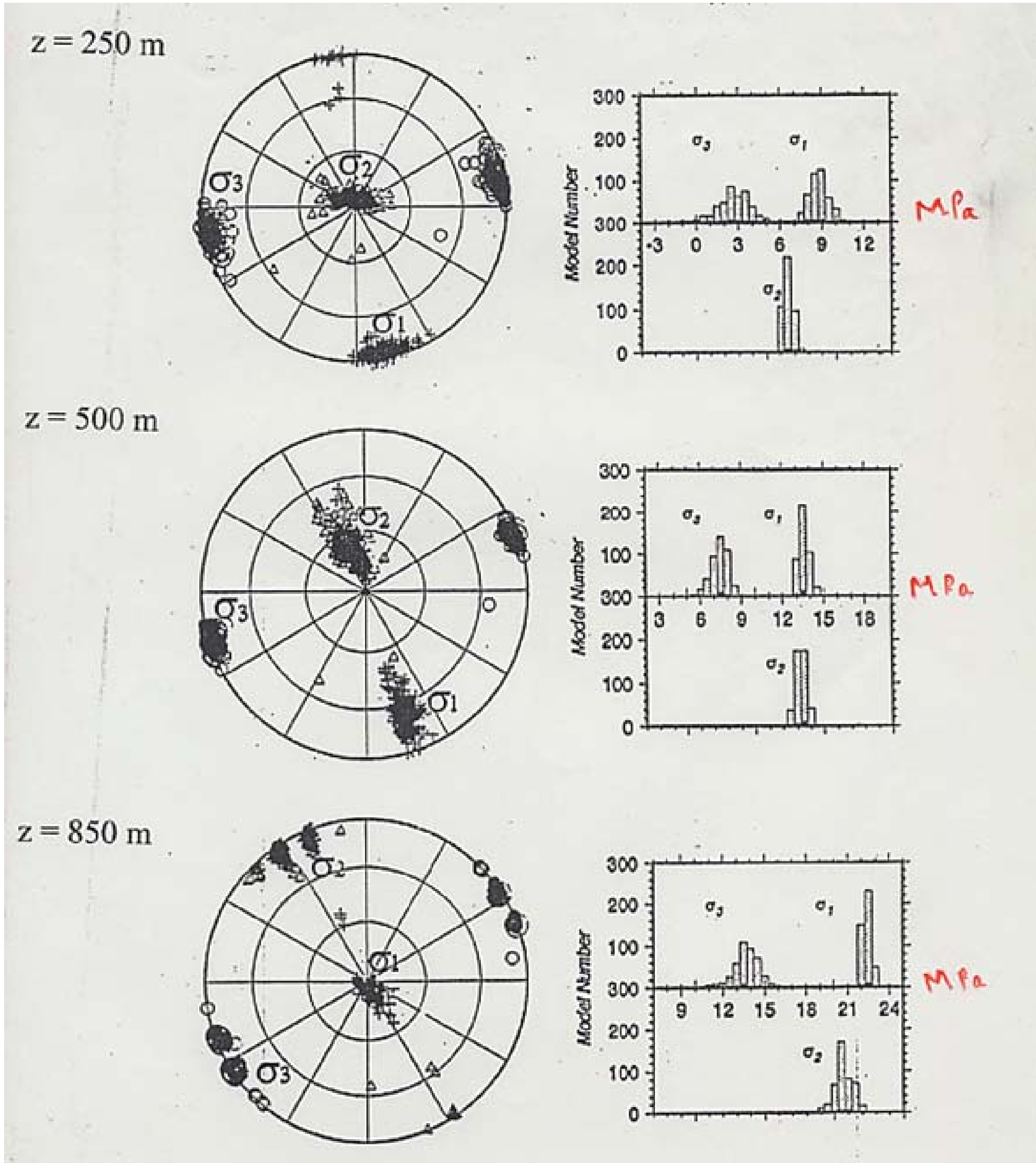

Using induced seismic events as pressure gauges

Coulomb's friction law : $\tau = \mu(\sigma_n - \alpha P) + C$

$P = Po + dP$, C# 0

α = pore pressure coefficient

P=pore pressure, Po=hydrostatic pressure,

dP = overpressure increment

$$dP = \frac{\sigma_n - \alpha Po}{\alpha}\left[1 - \frac{\tau}{\mu(\sigma_n - \alpha Po}\right]$$

Calibrating the friction law parameters - 1

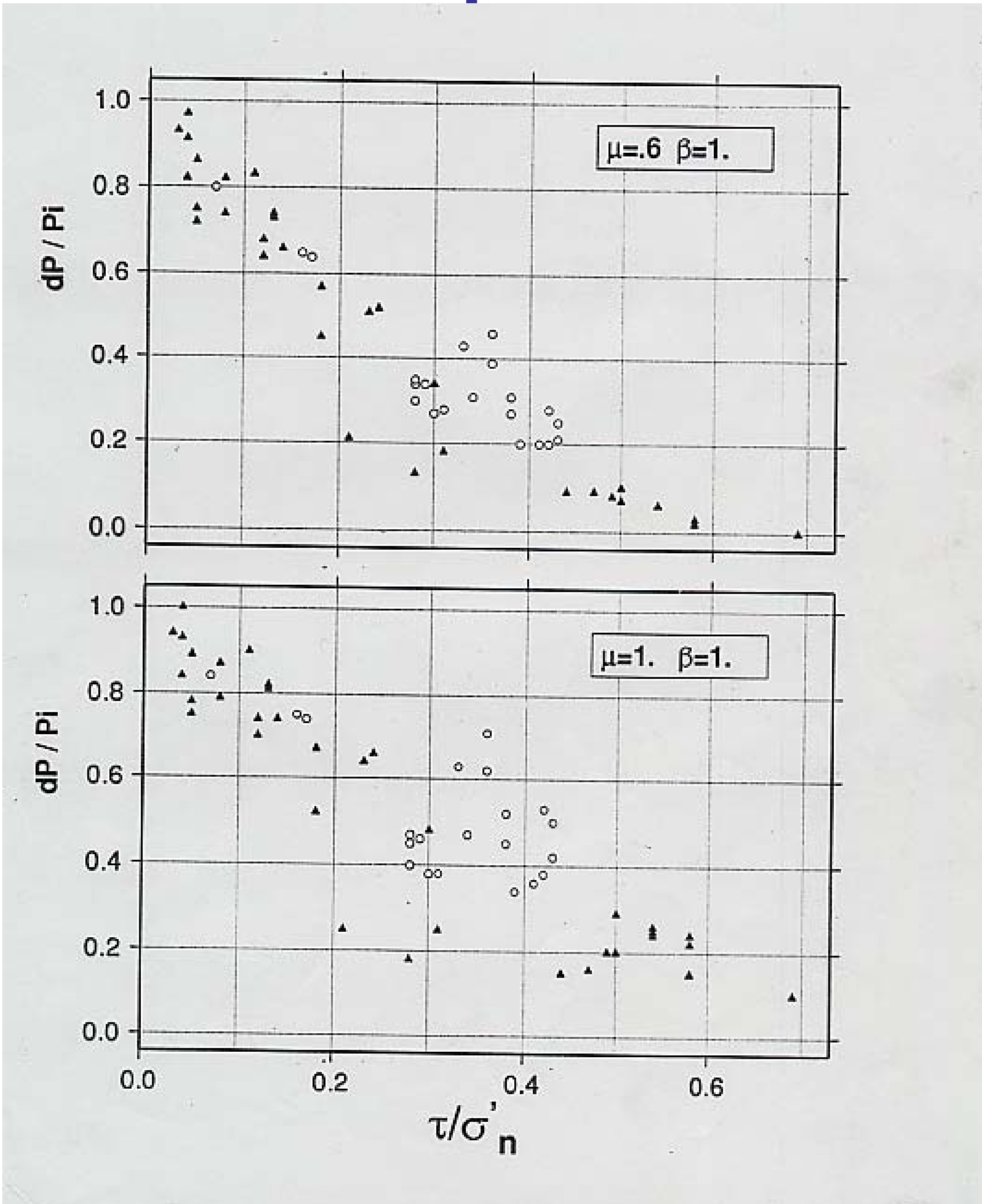

Calibrating the friction law parameters - 2

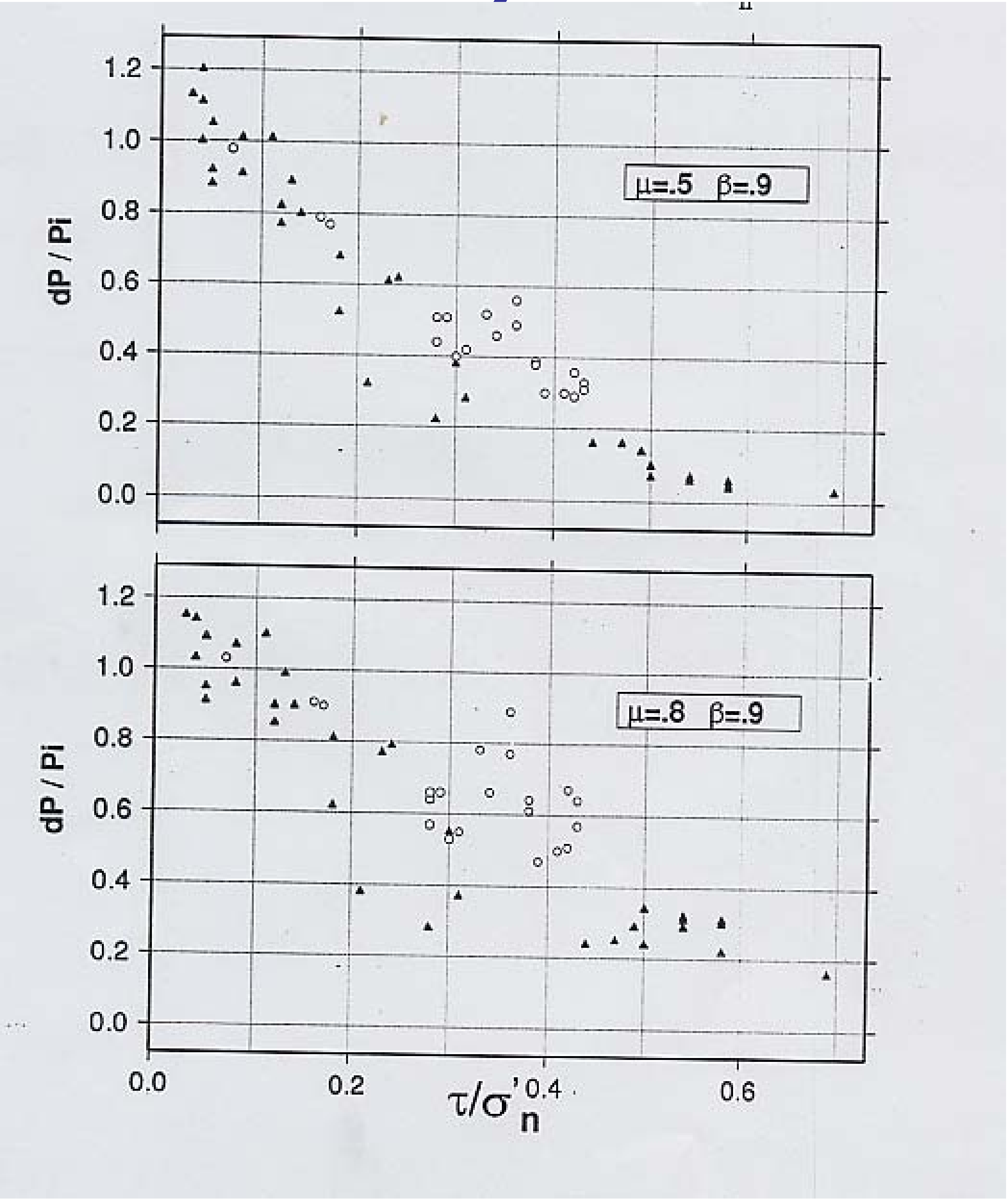

Mapping the pore pressure

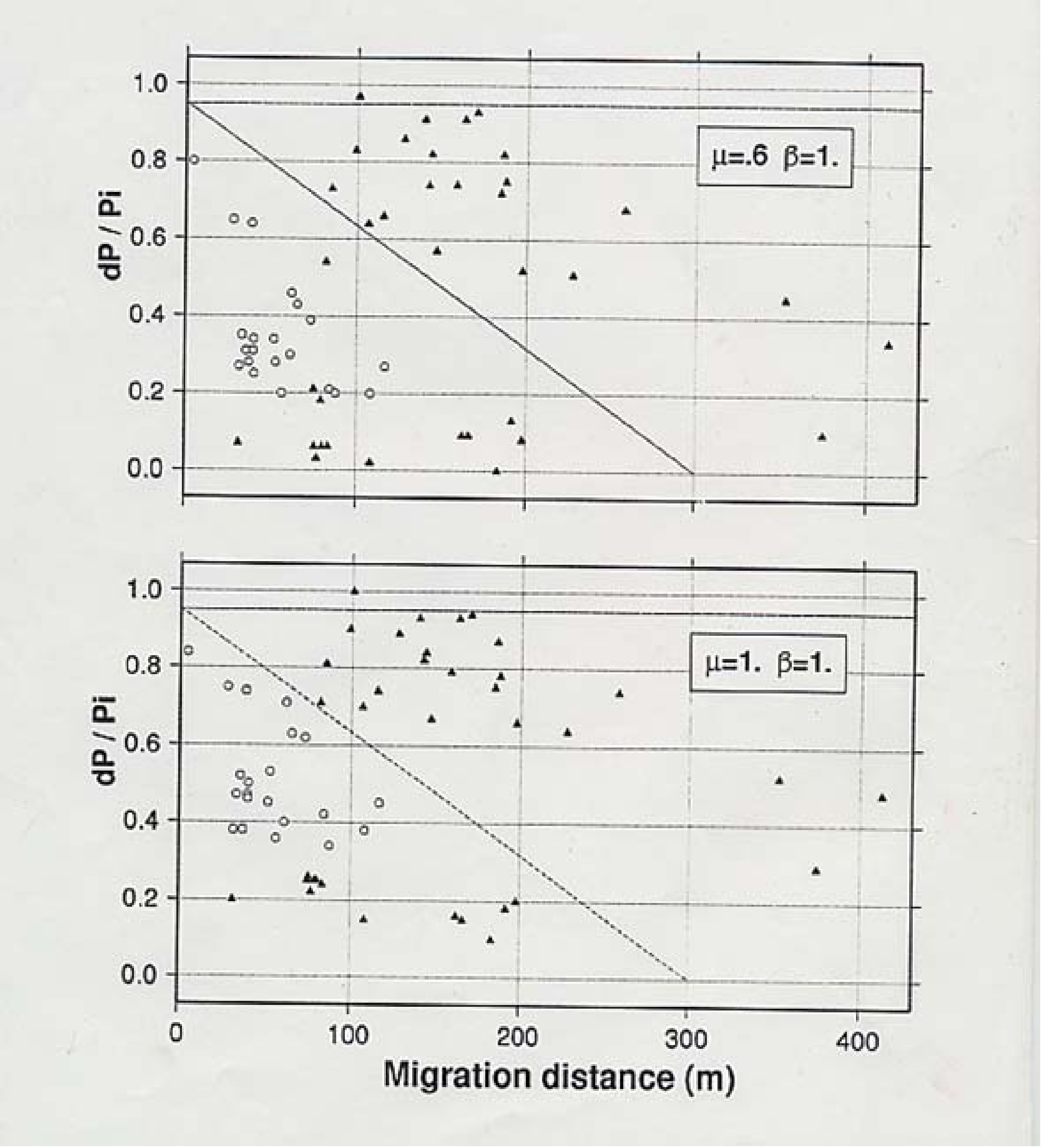

A simple explanation

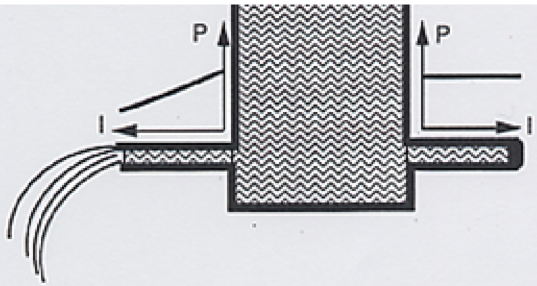

Flow through two parallel plates :

$$Q = \frac{e^3 w}{12m} \frac{dP}{dl}$$

Q -- flow rate
e -- hydraulic aperture
w -- fracture width
dP/dl -- pressure gradient
m -- fluid viscosity

Identifying flow zones from spinner logs

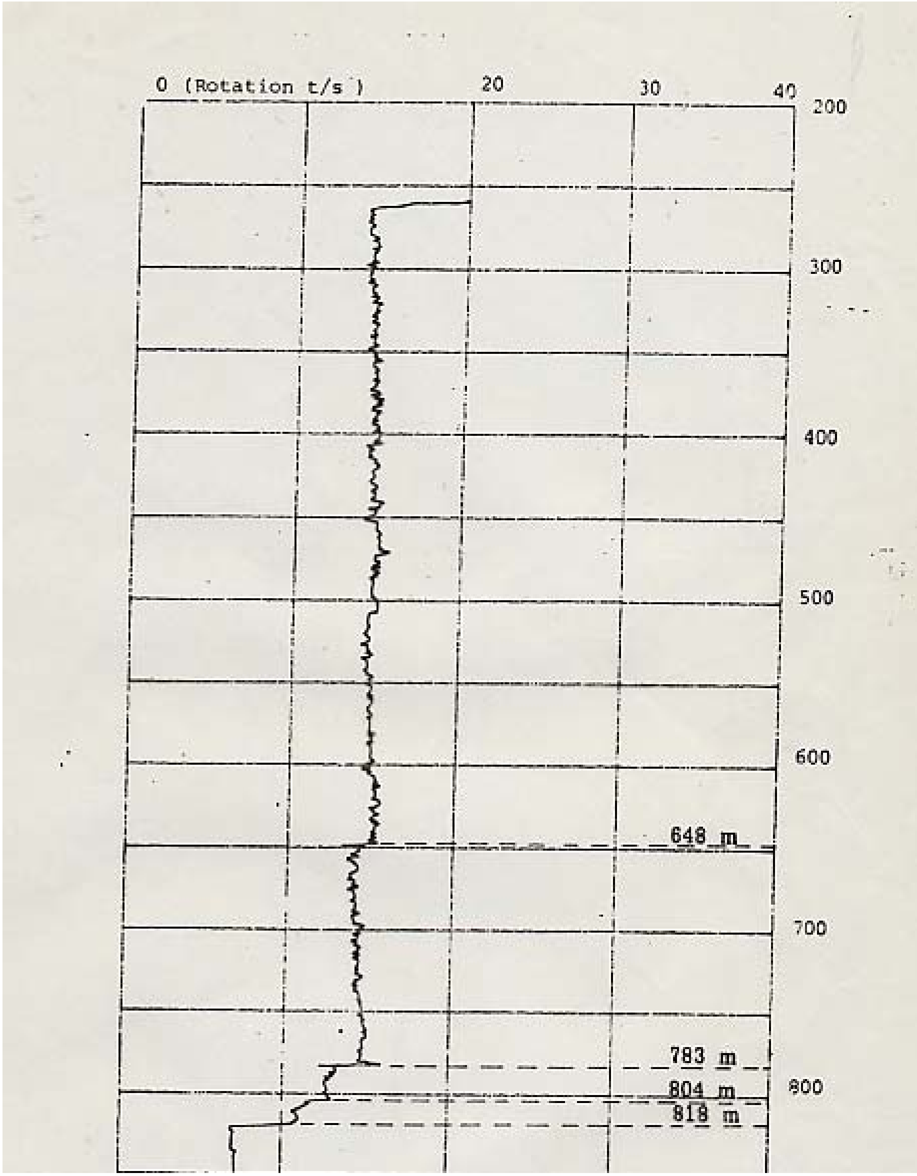

Conclusions from le Mayet de Montagne borehole tests

- Existence of stress heterogeneity, especially where flow occurs;
- Need to combine focal plane solutions with other data
- Induced seismicity maps high pore pressure, not high flow rate;
- All porous fracture zones may not be significant at the pluri hectometric scale

Philippine Fault

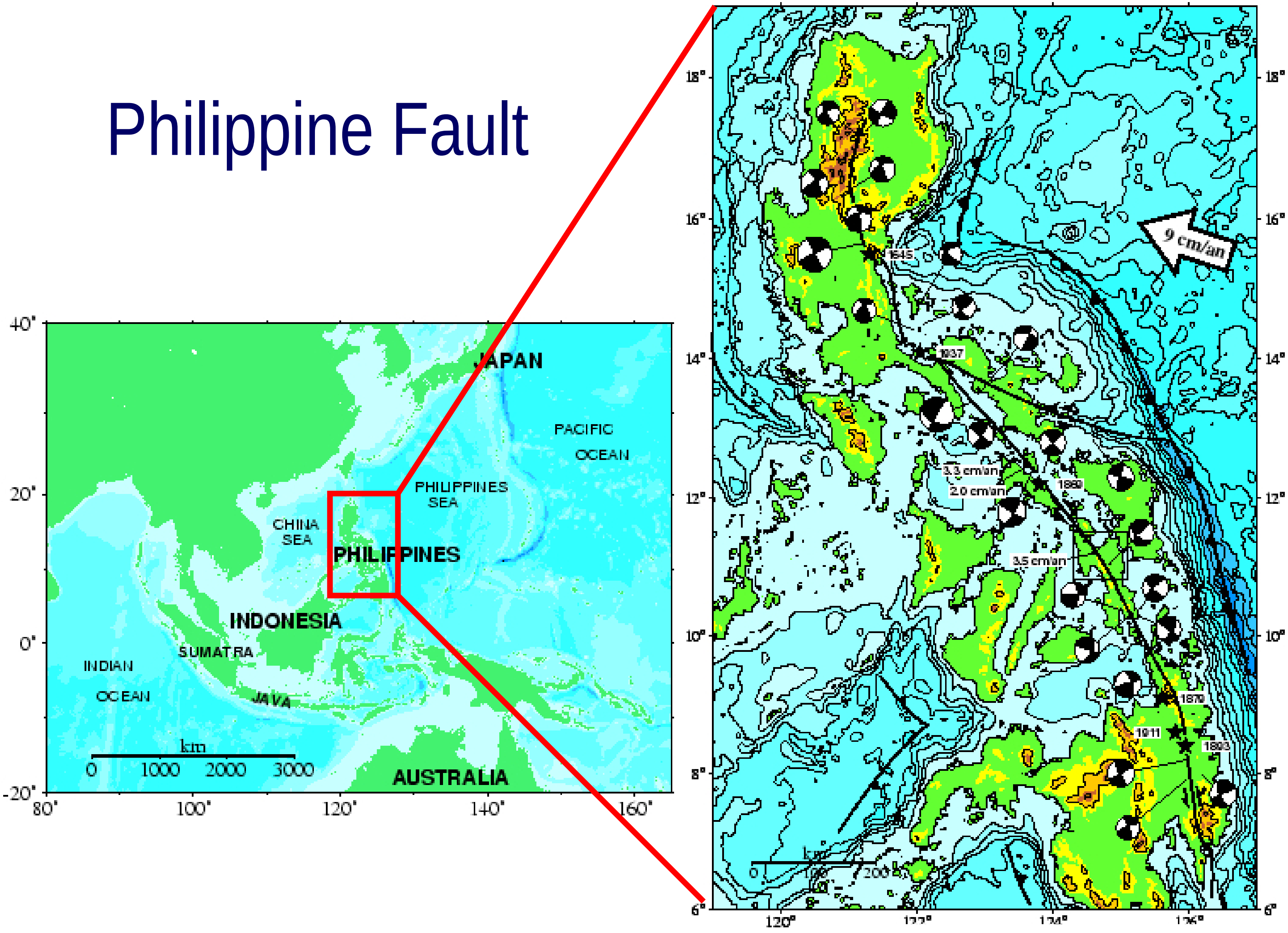

Philippine Fault on Leyte island

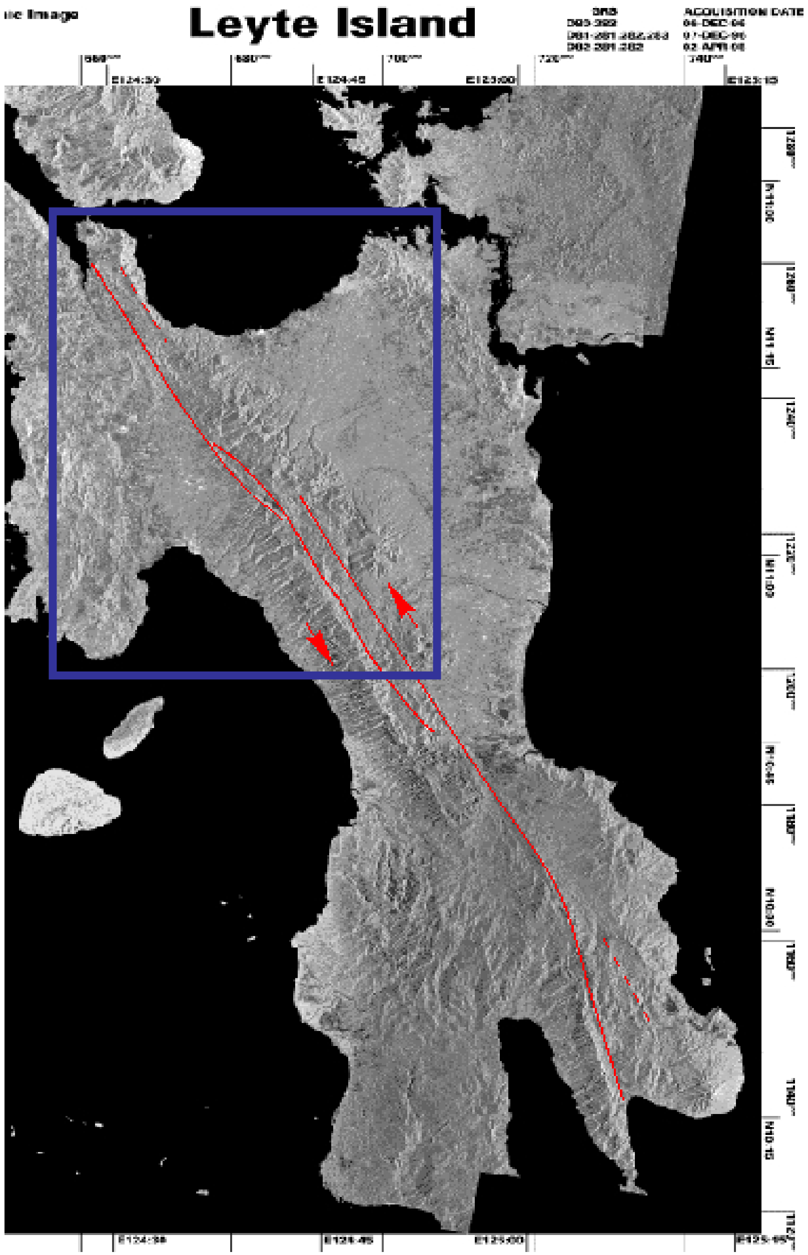

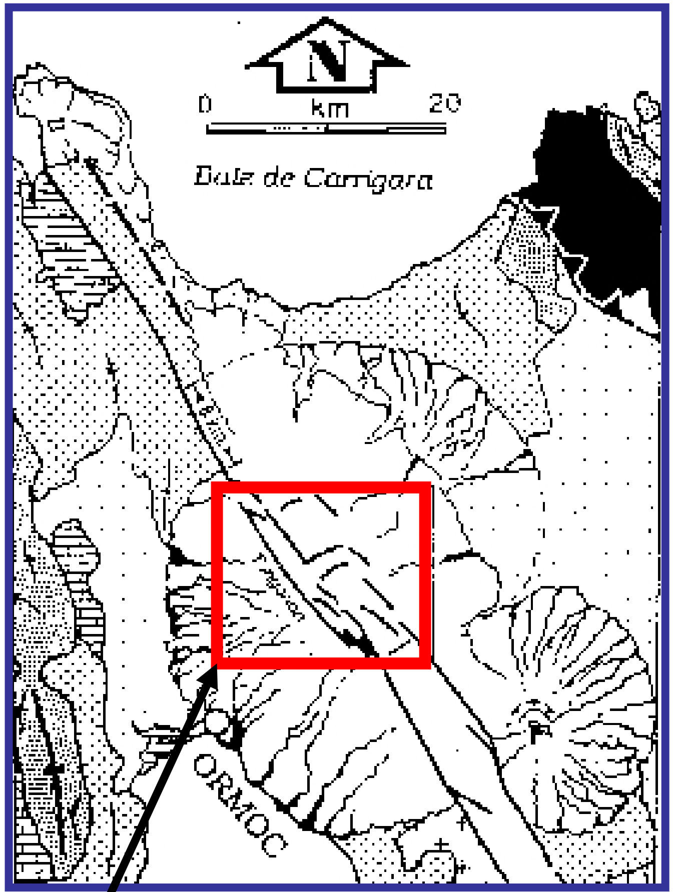

(Aurelio, 1992)

Tongonan geothermal field

Displacement field in the vicinity of the fault

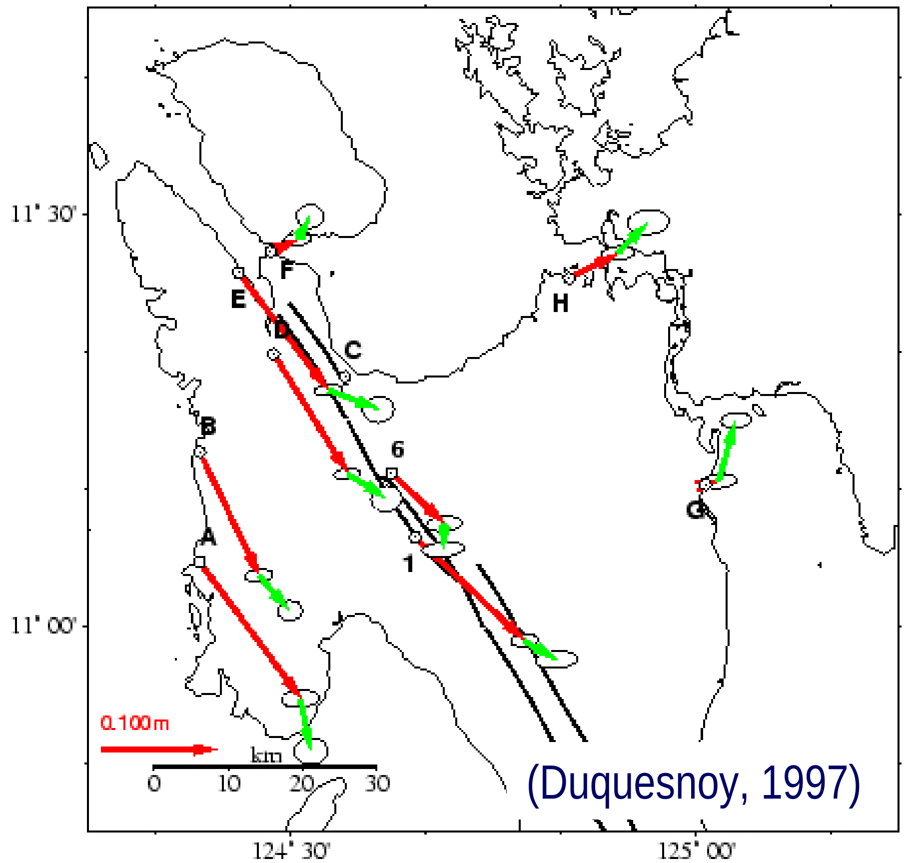

(Duquesnoy, 1997)

- GPS measurement 91-94-95
- 3.5 cm/y of creeping displacement

Seismicity

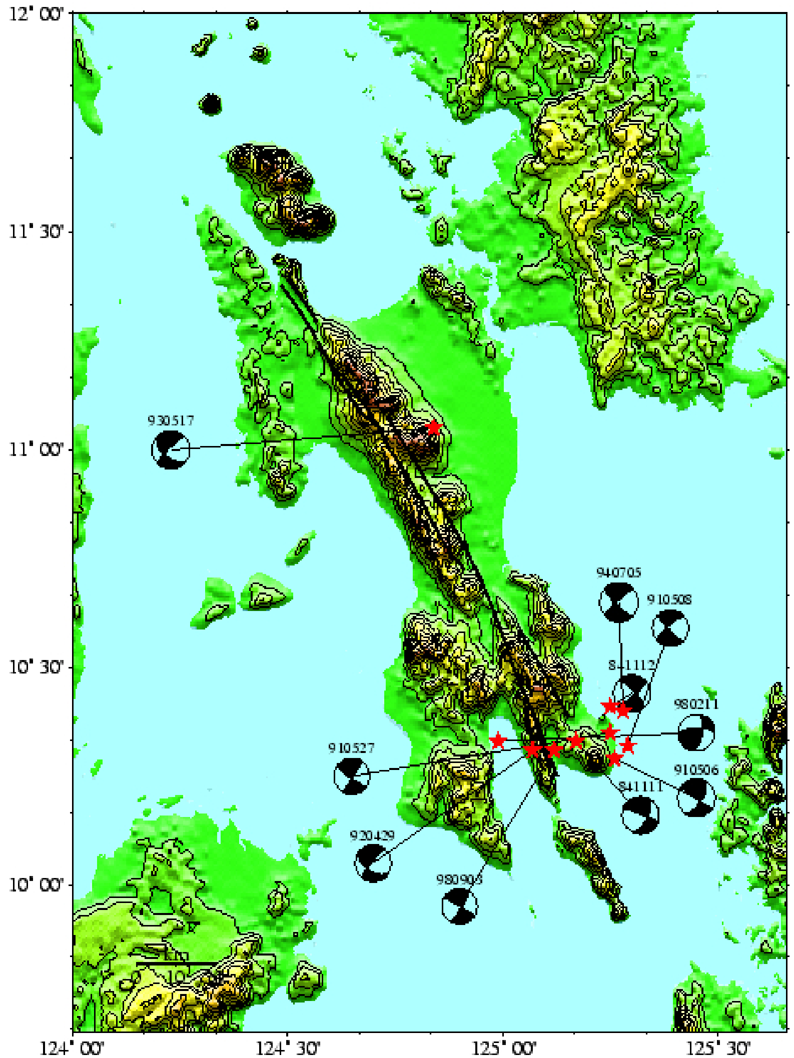

Displacement along the fault at Tongonan

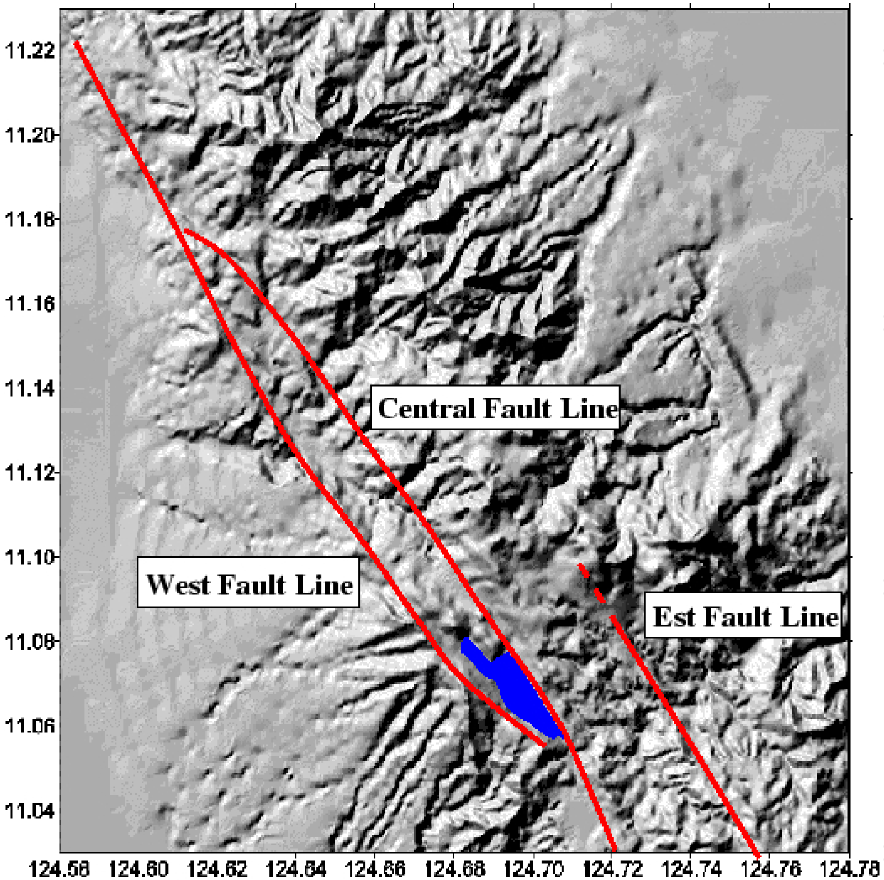

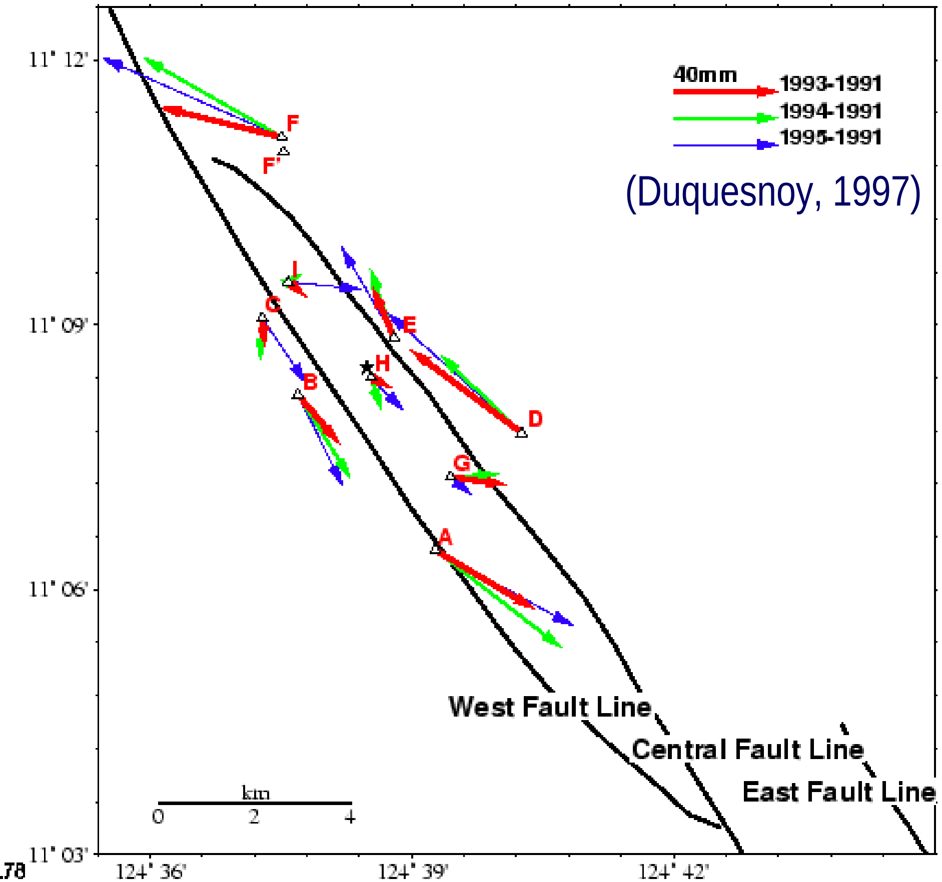

- Branches of Philippine Fault
- 2.4 cm/y of creep displacement

Injection experiment (1)

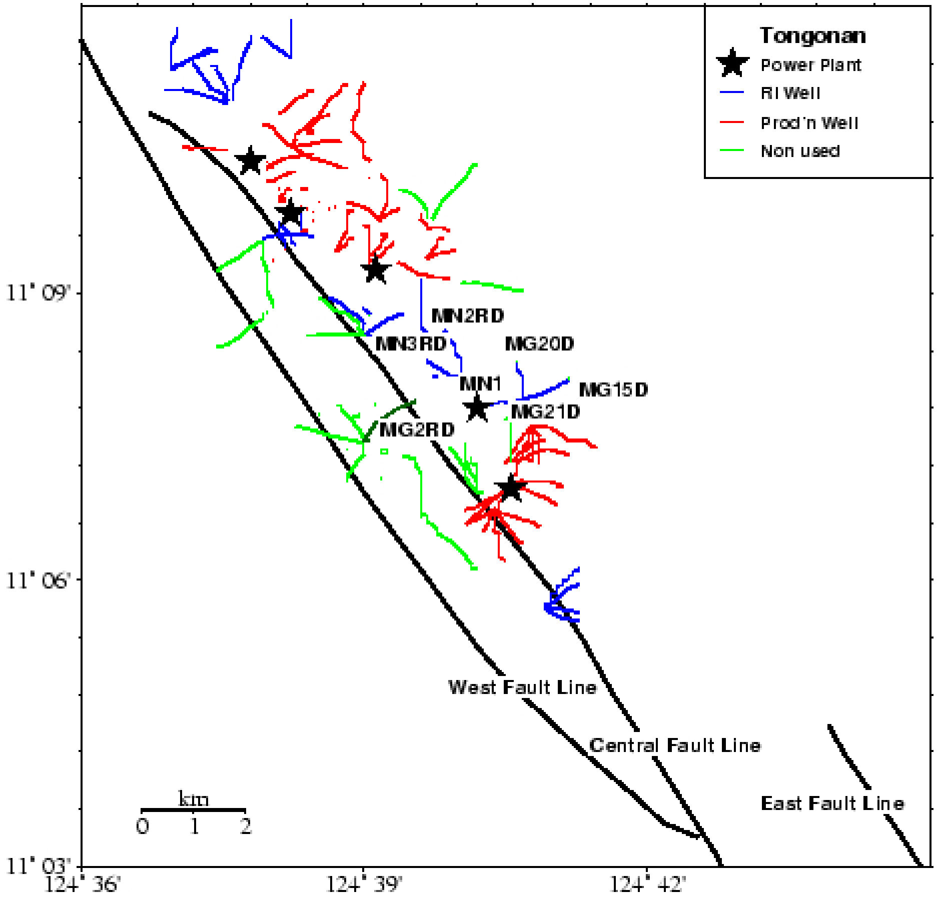

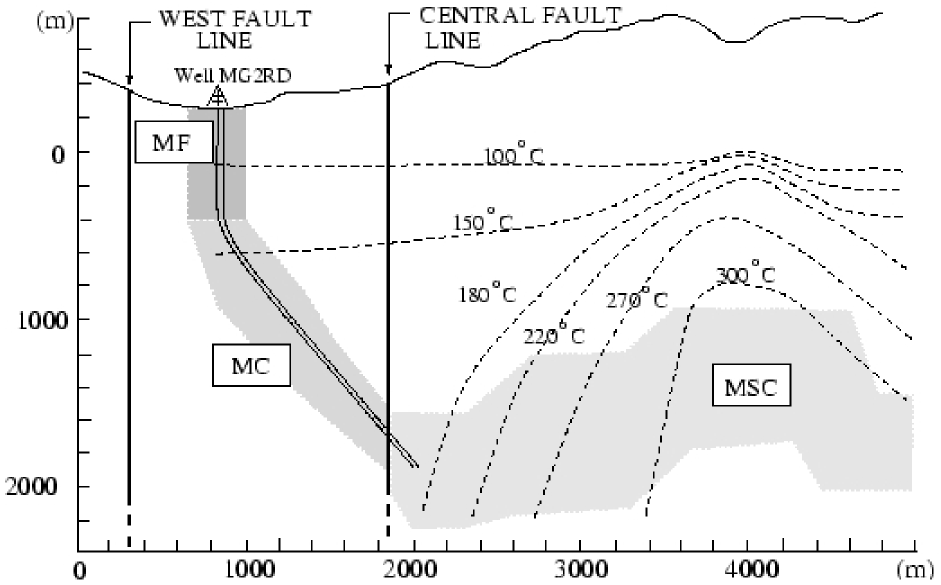

Injection experiment (2)

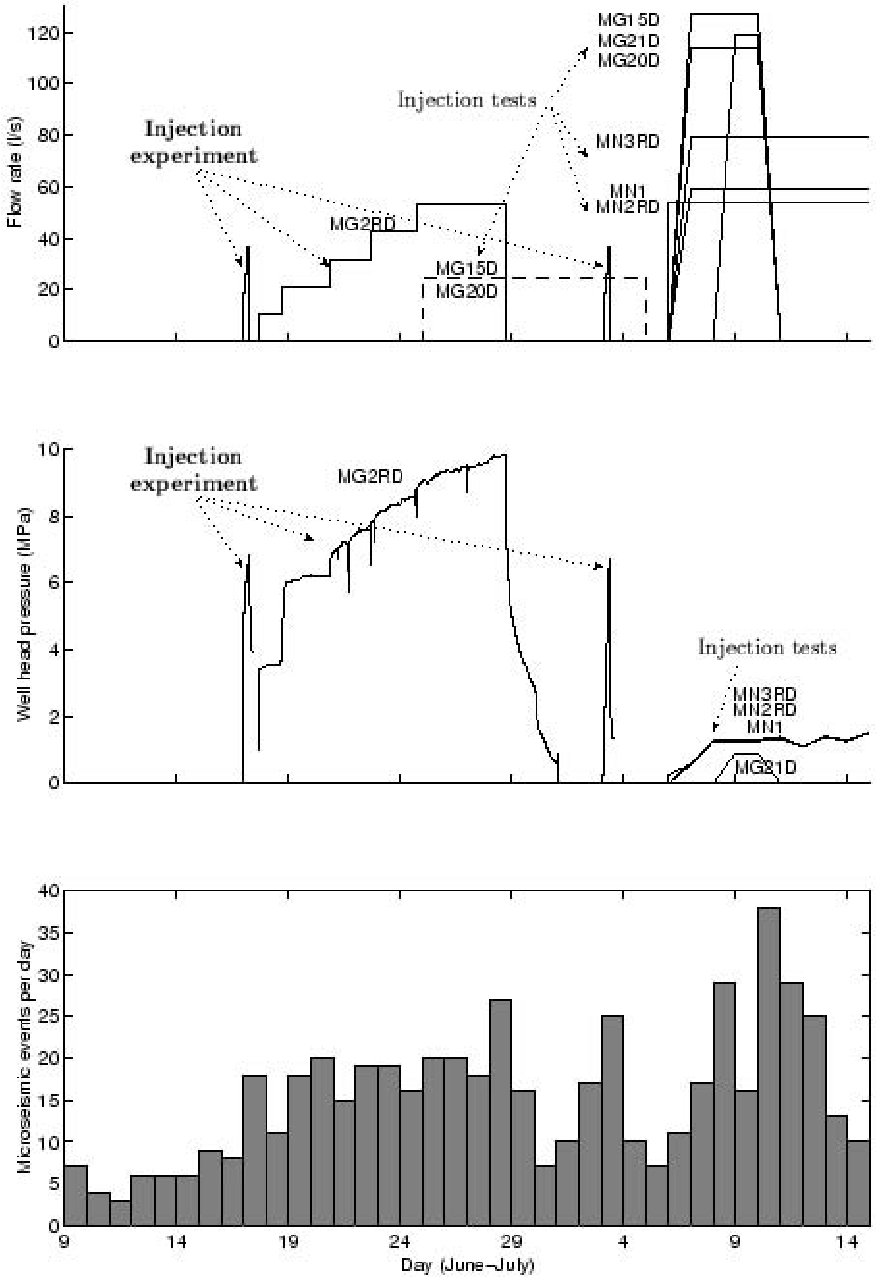

Injection experiment (3)

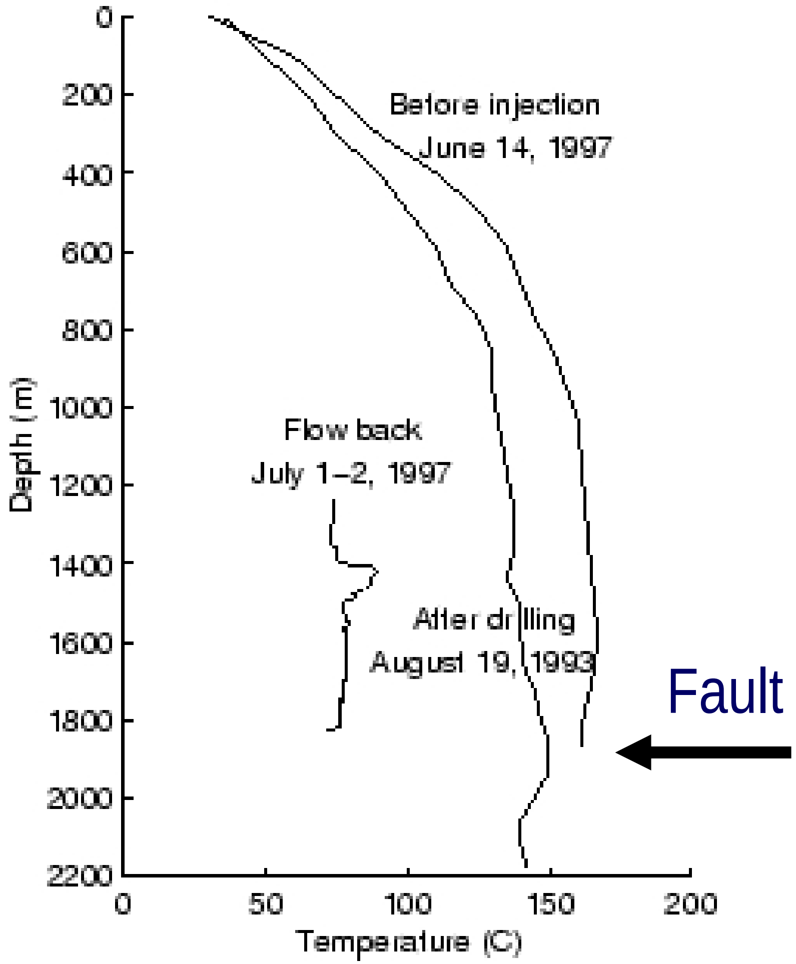

Summary of the observations:

- Water injected at the bottom of the well
- Well head pressure: up to 9 MPa
- Increase of microseismicity
- Injected volume: 36 000 m3
  (Other wells: 327 000 m3)

Seismicity acquisition

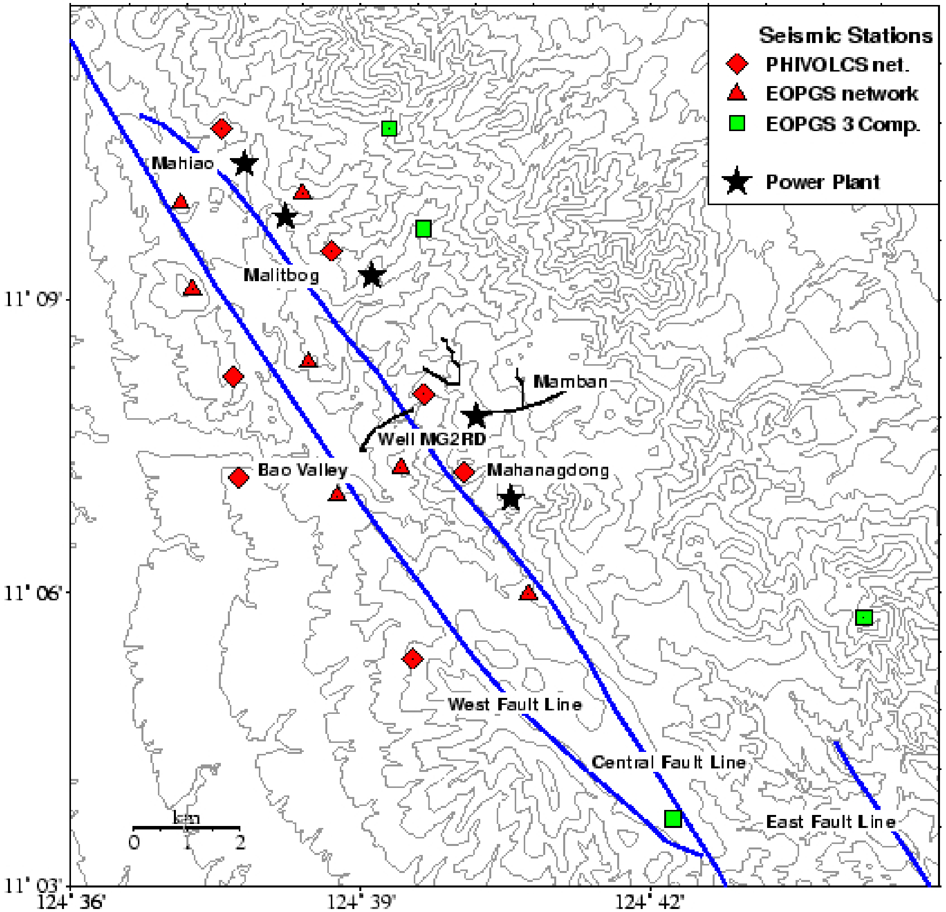

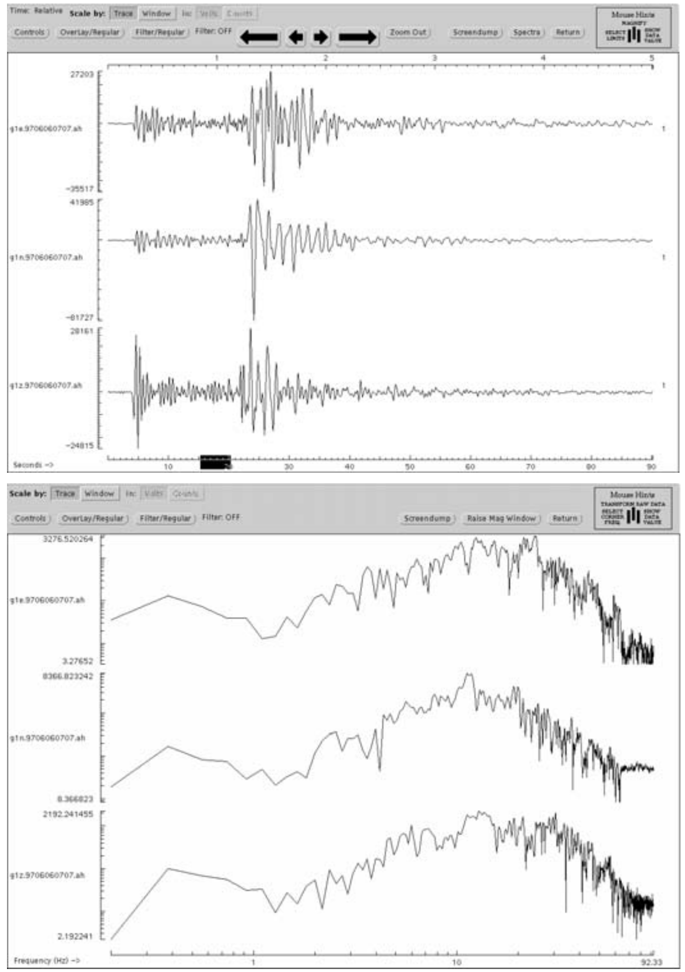

- Surface network (1-30 Hz)
- Feb. – Aug. 96 (Period 1) and Nov. – May 97 (Period 3): 7 stations
- Oct. – Nov. 96 (Period 2) and Jun. – Jul. 97 (Period 4): 18 stations (Four 3-C)

Tomographic inversion (1)

- Simultaneous determination of relocation and velocity model (Thurber, 1983)
- P and S traveltimes, 3-D grid with linear interpolation
- Iterative least squares inversion

Period 2: 141 ev. (1743 P, 1394 S) Period 4: 292 ev. (3939 P, 1352 S)

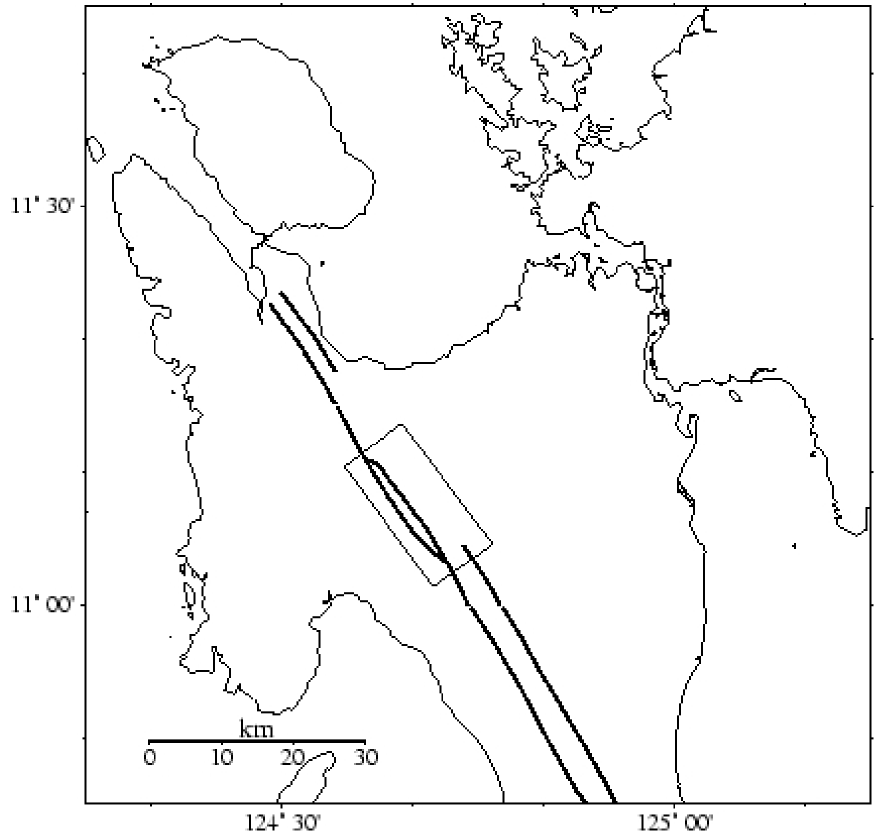

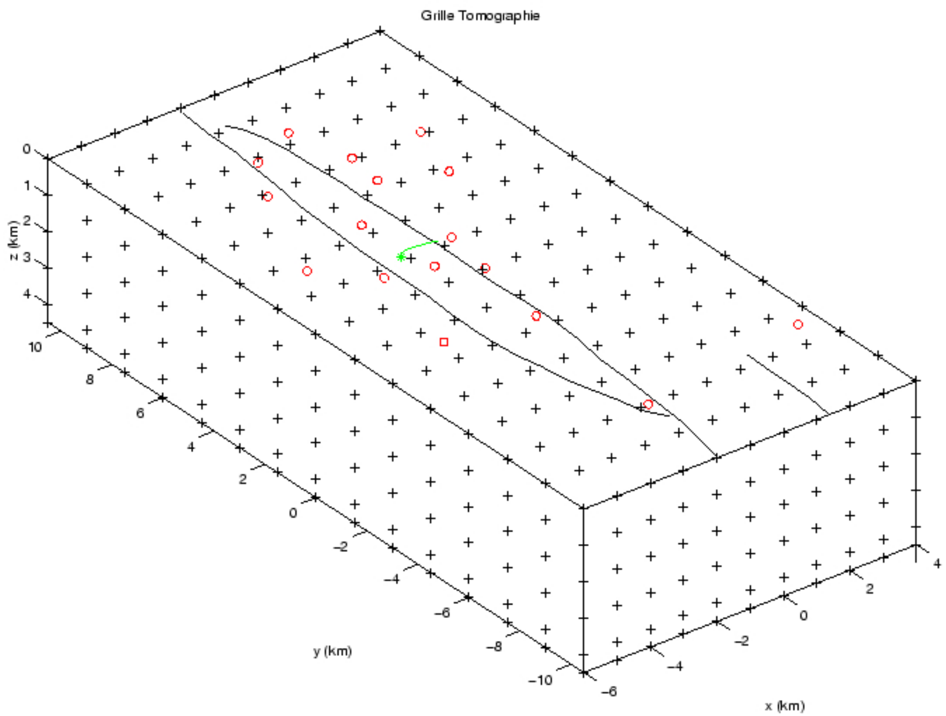

Induced microseismicity locations

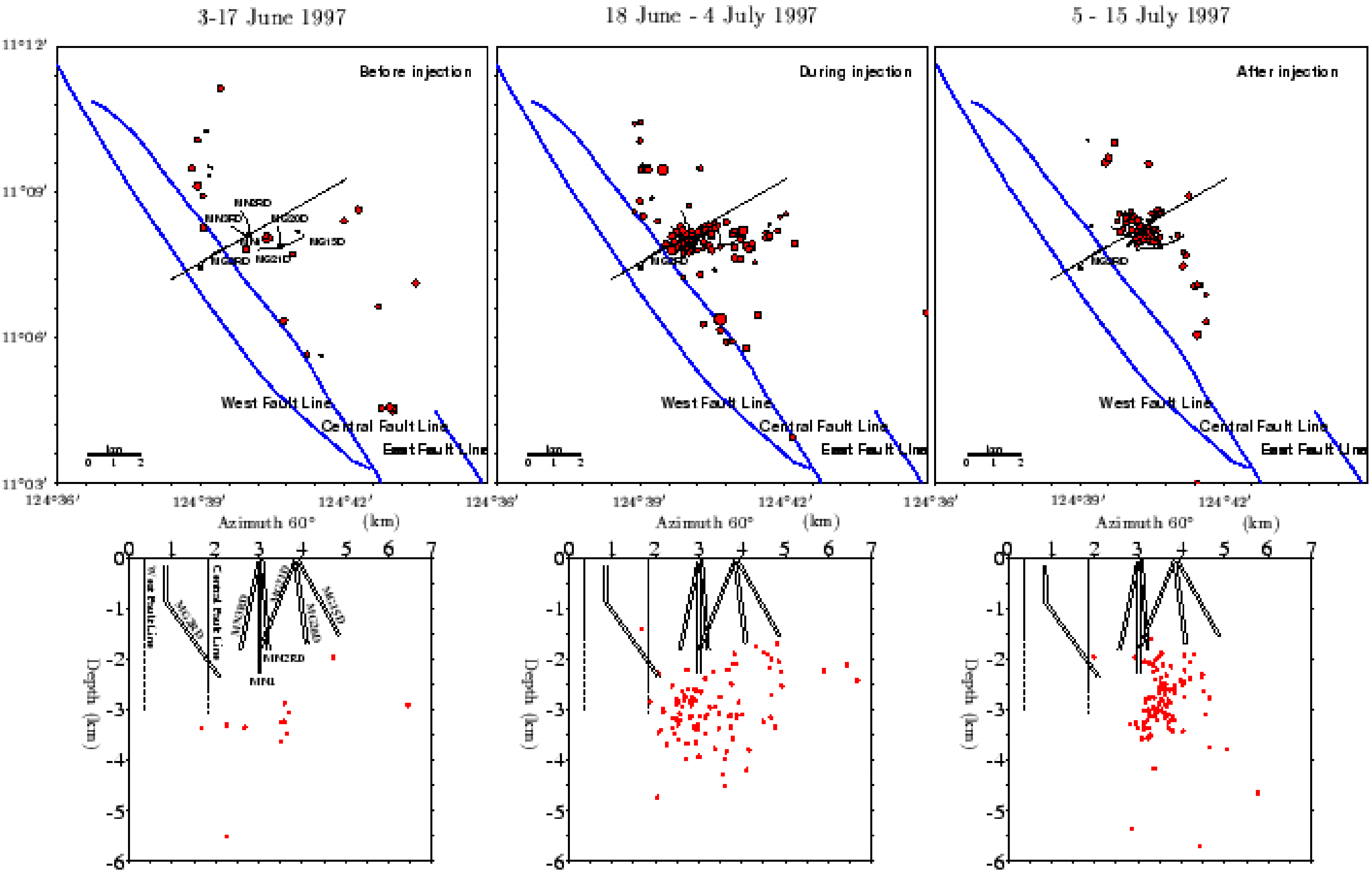

Seismicity relocations

Period 1+3 and 2

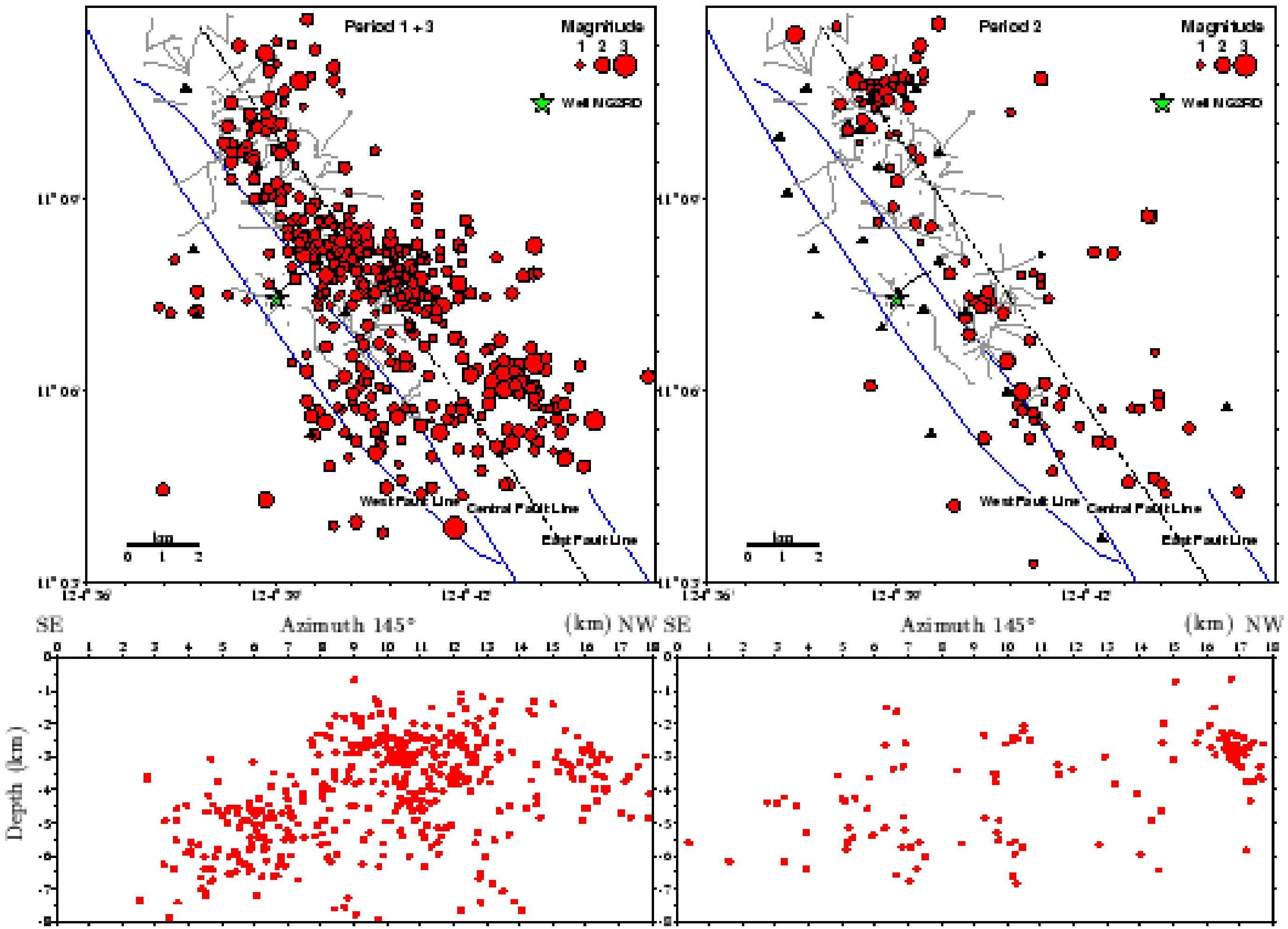

Vp velocity model (1)

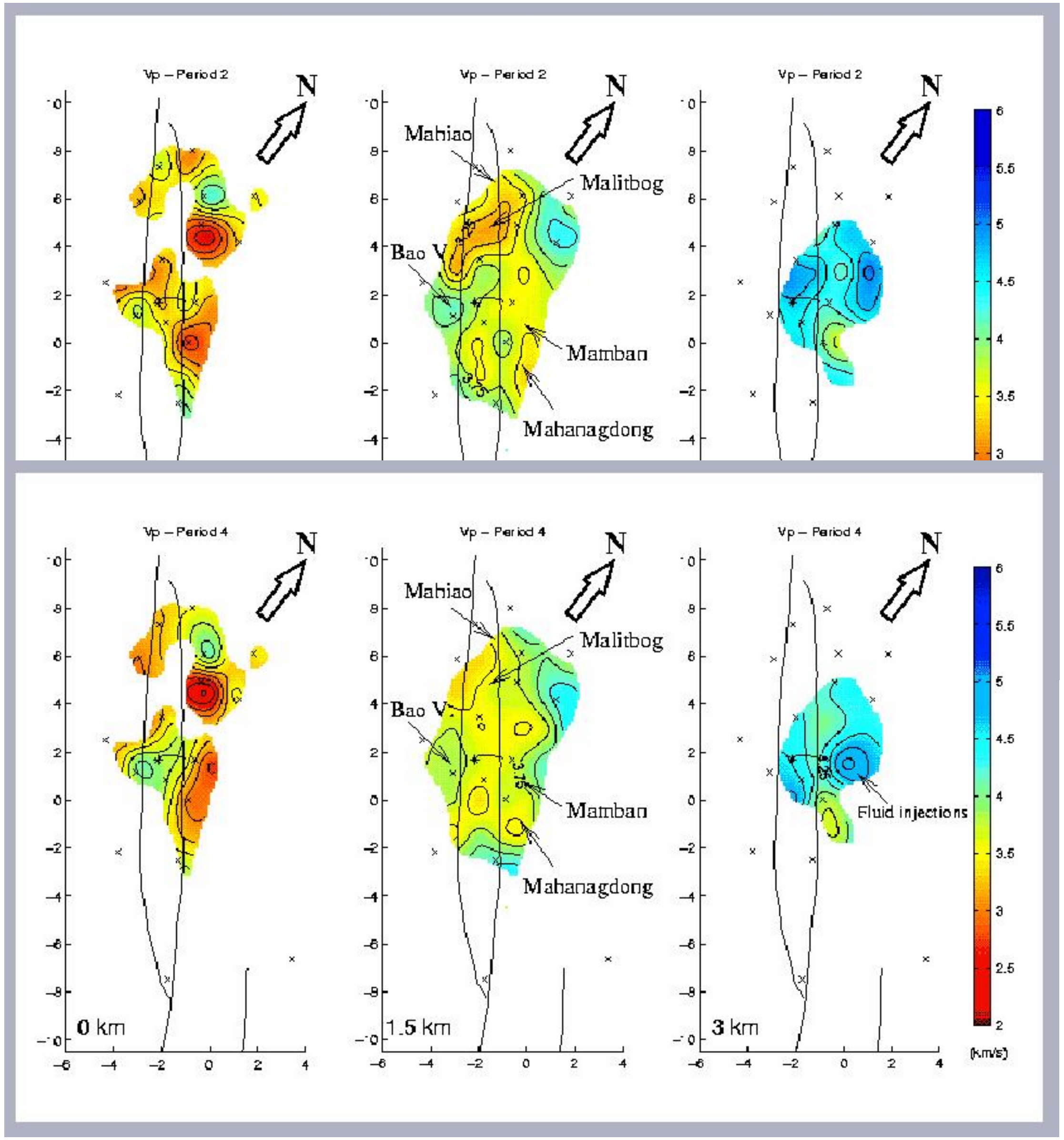

Before injection

After injection

Vp velocity model (2)

-before and during injection-

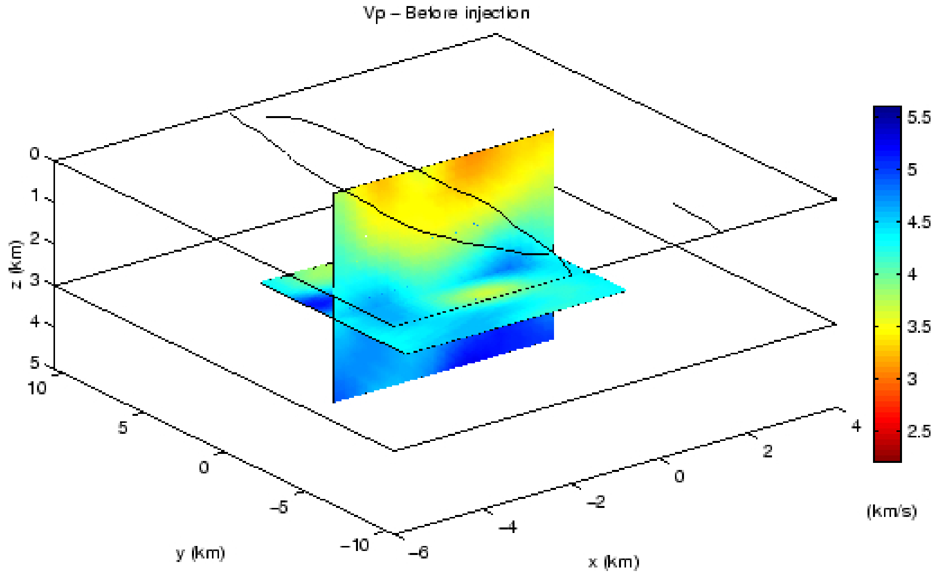

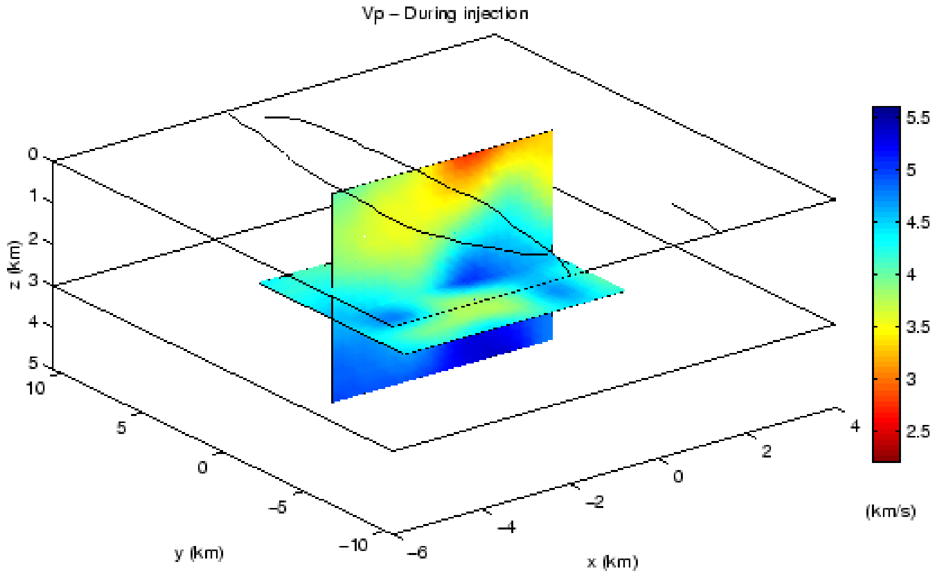

Focal mechanisms

Period 2

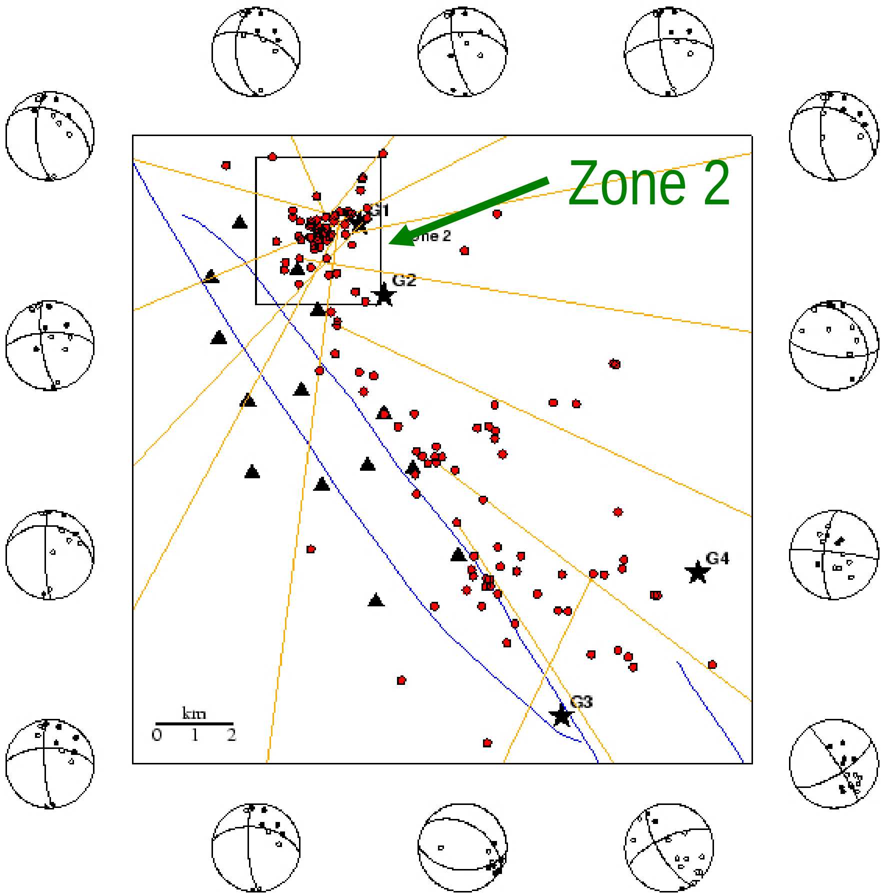

32 solutions

Period 4

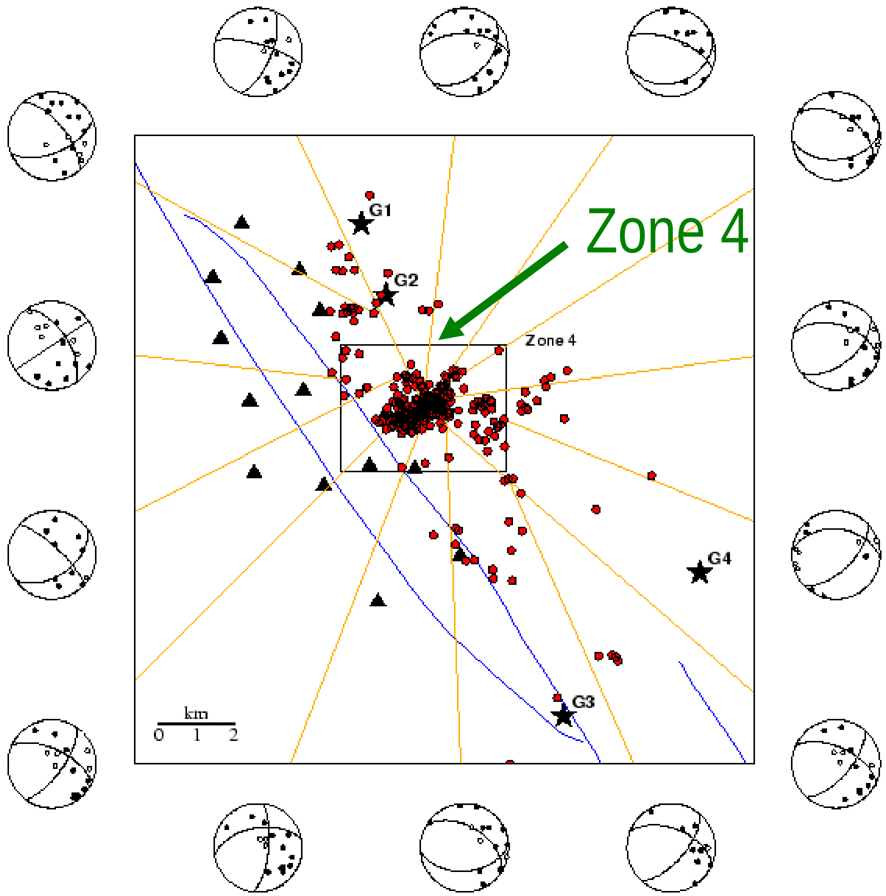

40 solutions

Focal mechanisms inversion

-first trial by zones-

Zone 2

23 focal mechanisms

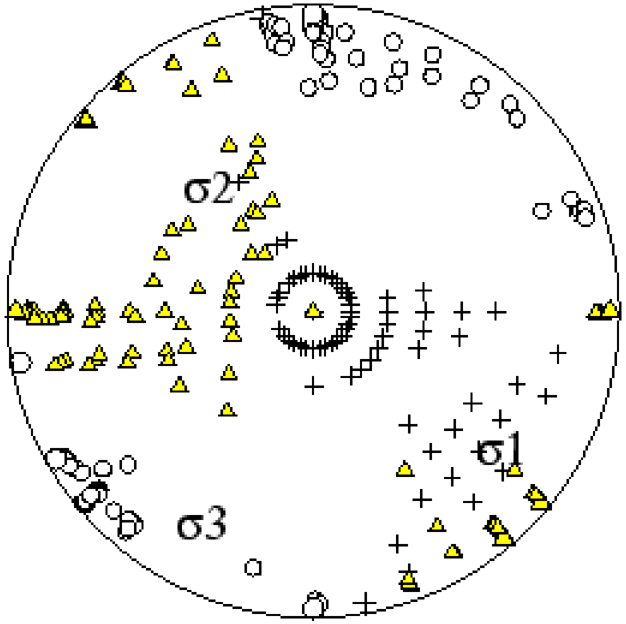

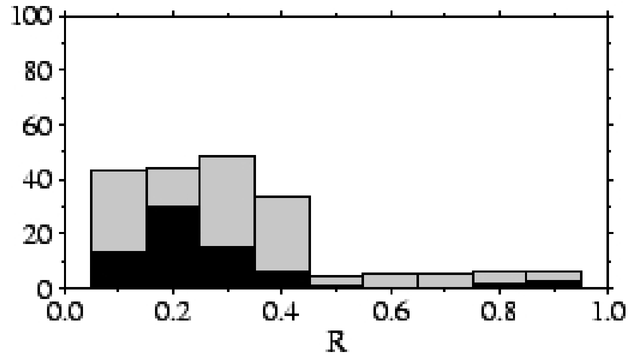

Solutions in 90 % confidence domain

Best solution compatible with 83 % of the data

Zone 4: no solution

Principle of shear wave splitting

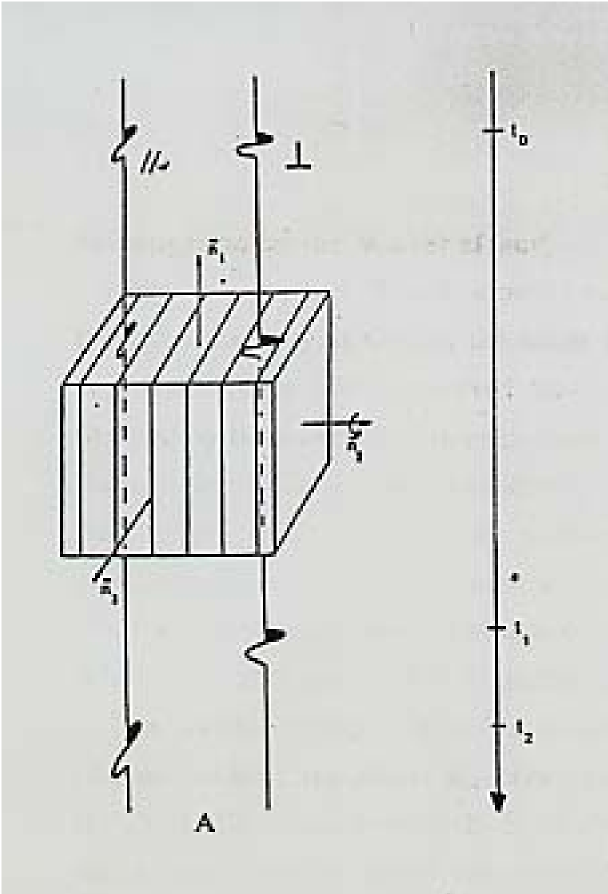

- In anisotropic materials shear wave velocity varies with direction leading to shear wave splitting. .
- In planar isotropy, 5 elastic constants.
- waved polarized parallel to plane are faster.

Fast S- wave polarisations

-Period 2 and 4 -

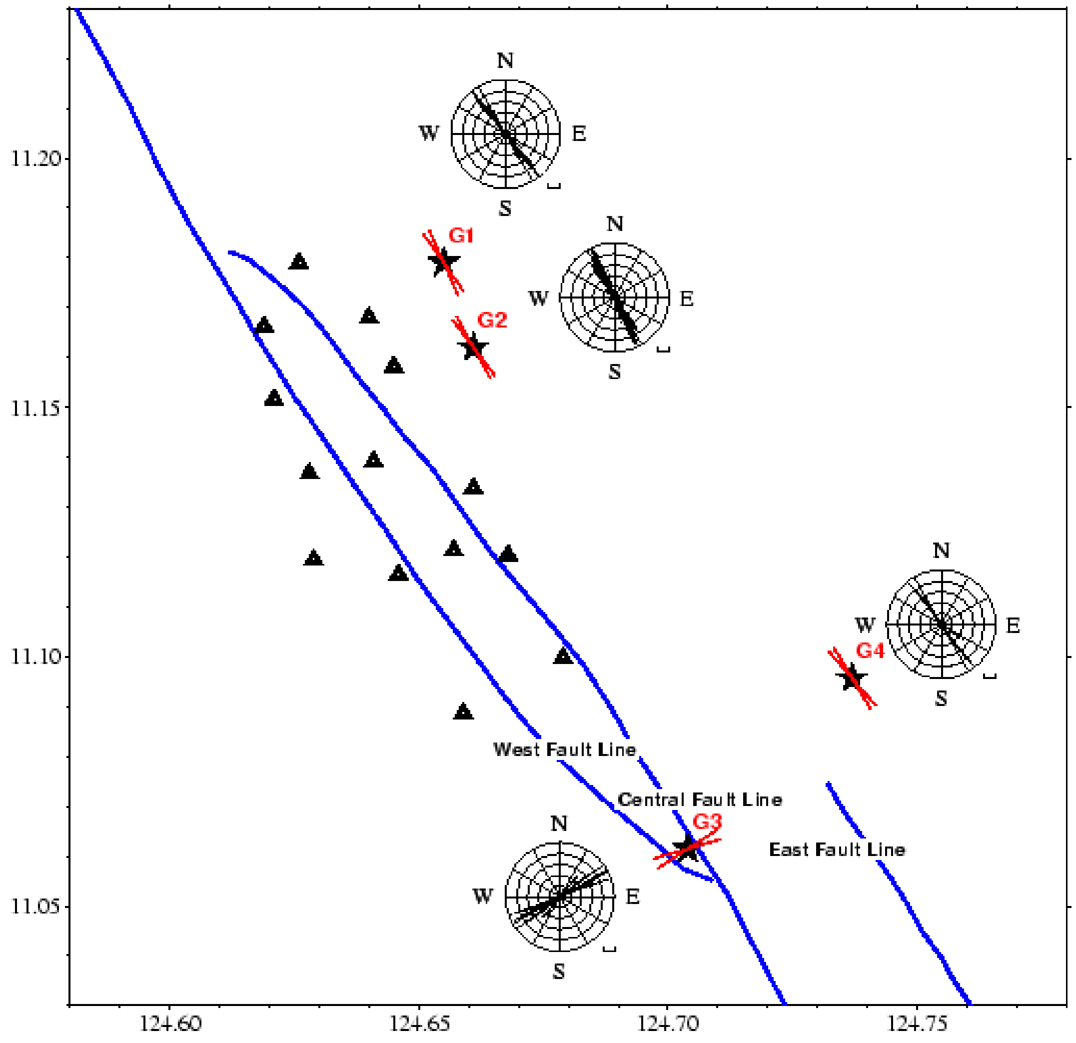

- Shear wave splitting
- G1, G2, G4: parallel to fault
- G3: orthogonal to fault

Stress heterogeneity in the seismicity cloud?

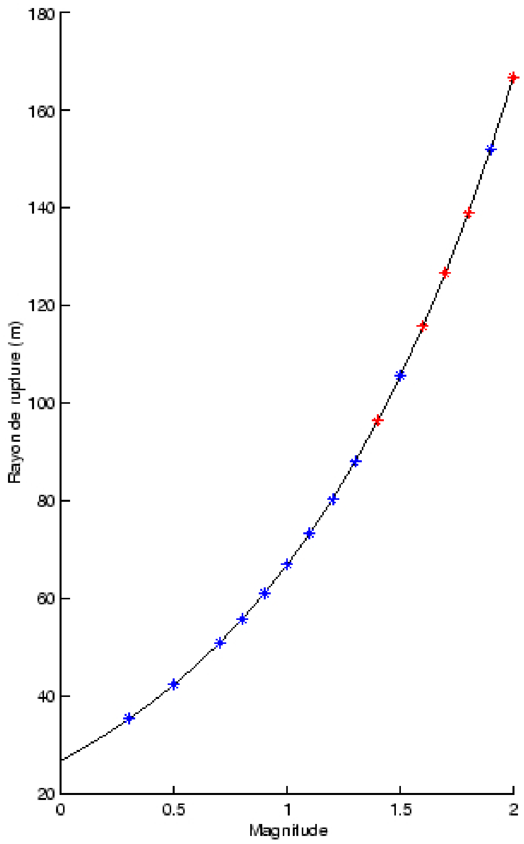

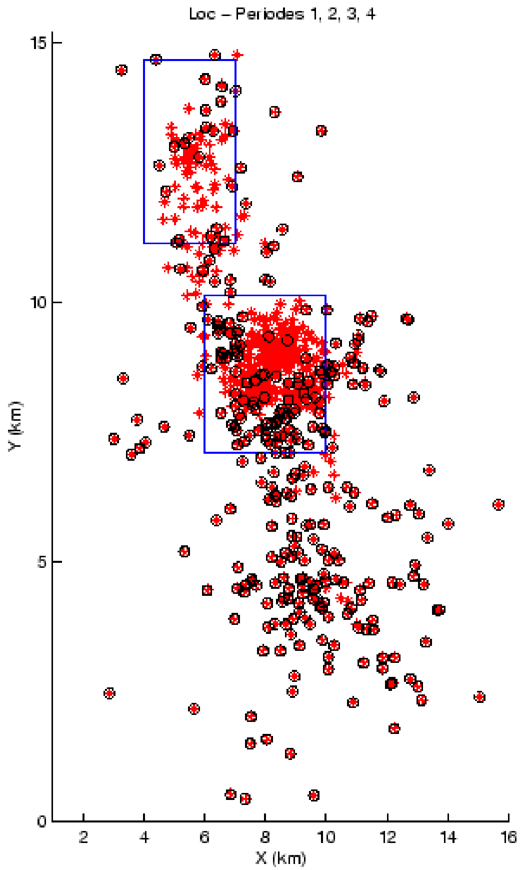

New data selection:

- Definition of a sphere for each event with radius~rupture dimension
- Successive events with intersecting spheres are excluded

Focal mechanisms inversion

-new data selection-

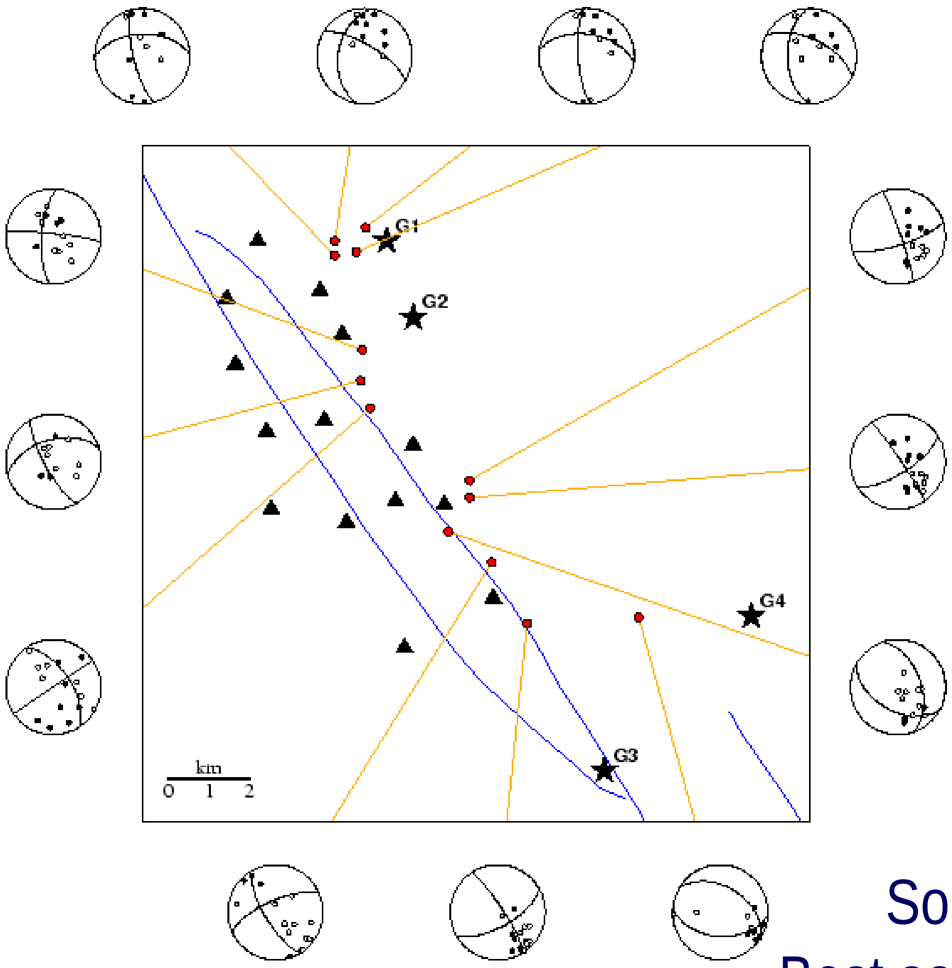

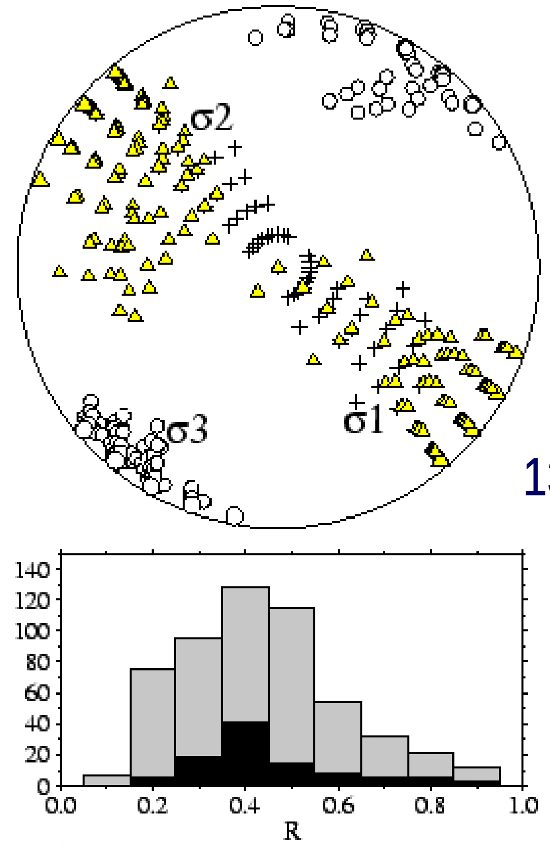

13 foc. Mech.

Solutions in 90 % confidence domain

Best solution compatible with 91 % of the data

Fast S- wave polarisations

-east of the Central Fault (G1, G2, G4) -

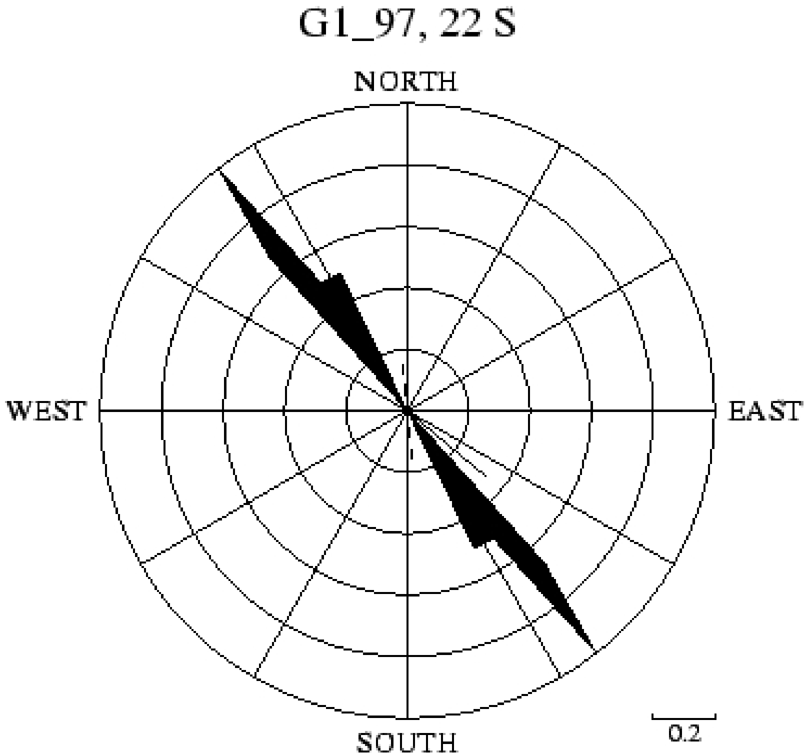

Fast polarisation ~ 145 deg.

Inversion focal mechanisms

-new selection-

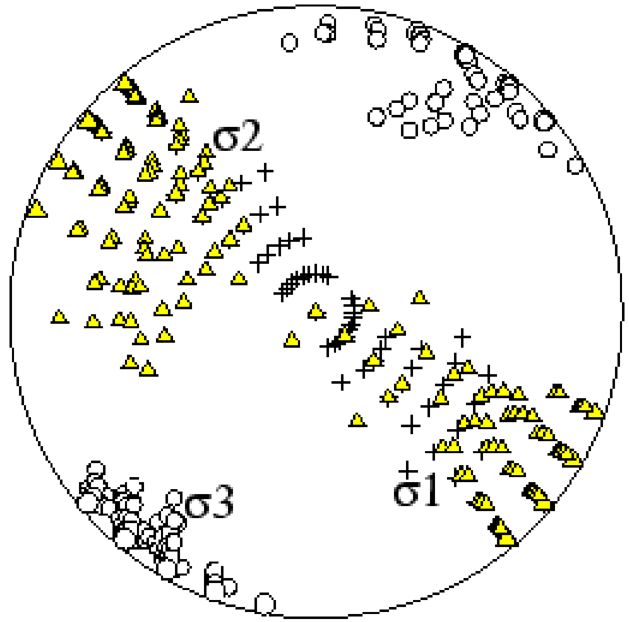

$\sigma 1$ and $\sigma 2$ ~ 110-150 deg.

Observations compatibility in regional context

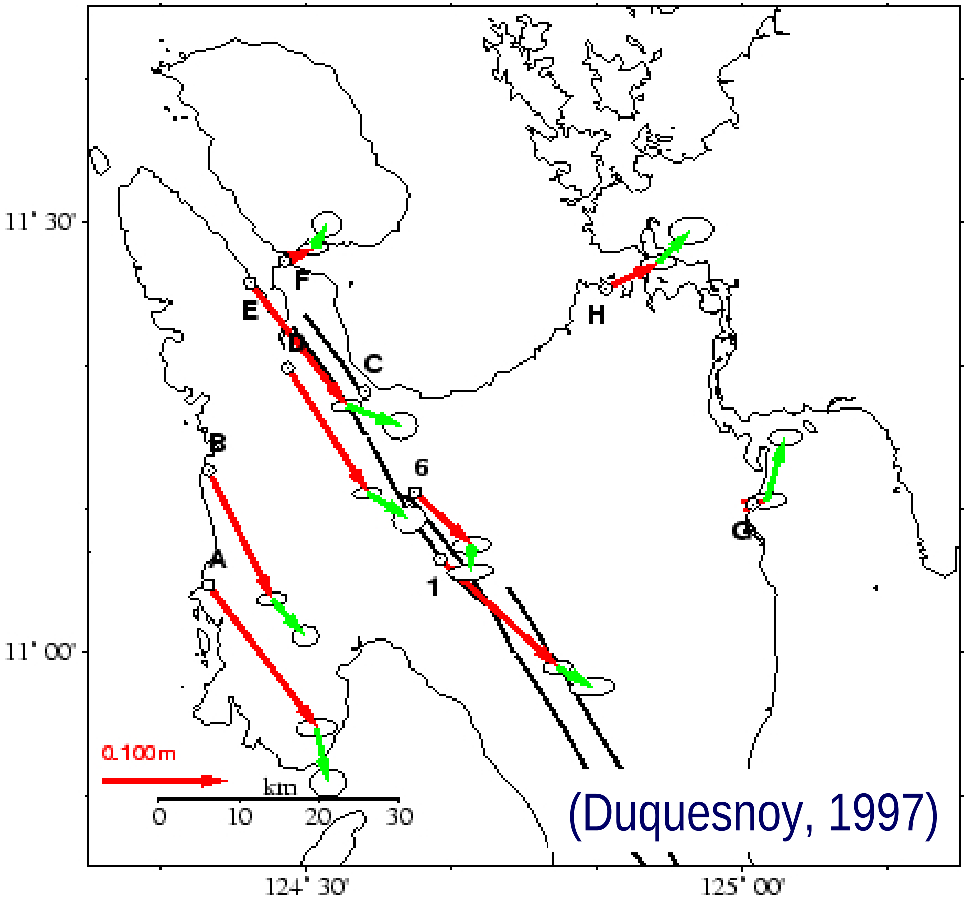

- Minimum principal stress orthogonal to fault
- GPS data show extention orthogonal to fault ~0.6-1.8 cm/y

Extension basins along the fault

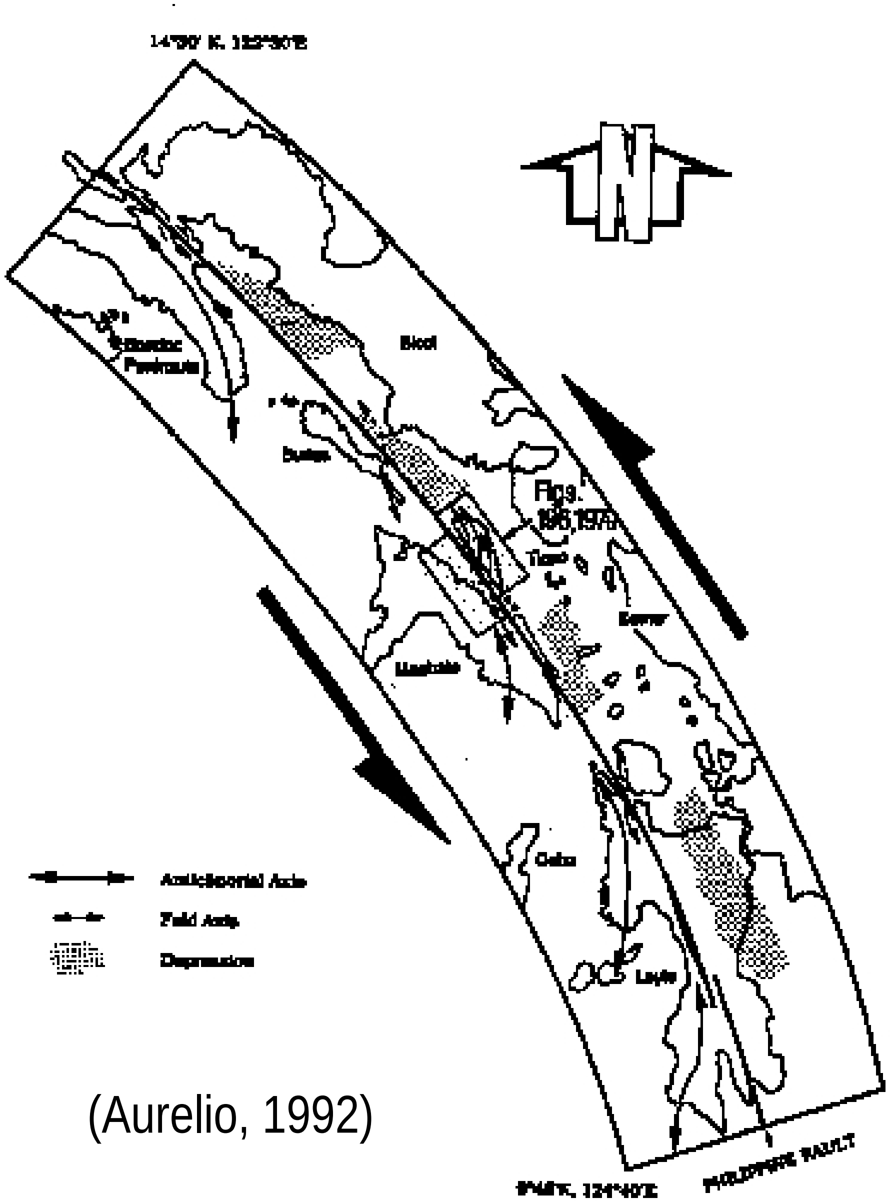

(Aurelio, 1992)

Conclusions from Tongonan experiment

- Effect of interactions between events, but once independent events are selected, results are consistent with shear wave splitting conclusions

- Shear wave splitting yields consistent results

- Fault is normal to principal stress direction and therefore does not support, locally, any shear stress component